Theory and Simulation of Equatorial Plasma Bubbles and Scintillation

John Retterer

Institute for Scientific Research

Boston College

BOSTON COLLEGE ISR INSTITUTE FOR SCIENTIFIC RESEARCH

13 October 2022

Theory and Simulation of Equatorial Plasma Bubbles and Scintillation

- Connection between Equatorial Plasma Bubbles (EPBs) and Scintillation
- Fluid plasma turbulence
- Physical mechanism – interchange instabilities
- Influence of the dynamics of the lower atmosphere and the magnetosphere
- Model equations
- Example simulation
- Scintillation from bubble calculation
- Bubble and scintillation climatology
- Post-midnight bubbles over Africa
- Parameter sensitivities
- Prospects for forecasting

Equatorial Scintillation

Associated with Plasma Depletions

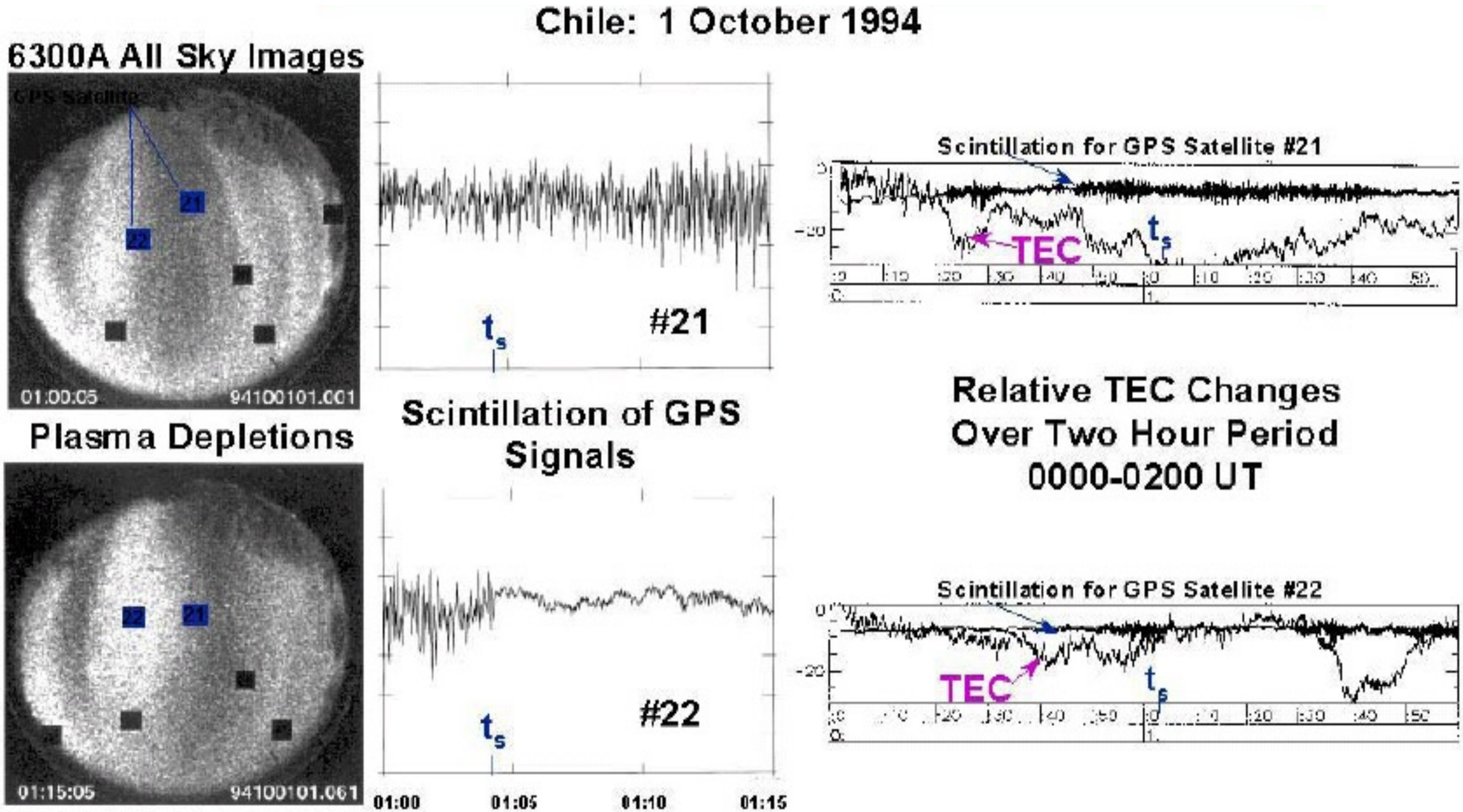

Plasma Turbulence

Observed Density Irregularity Spectrum

Rocket fly-through density measurements

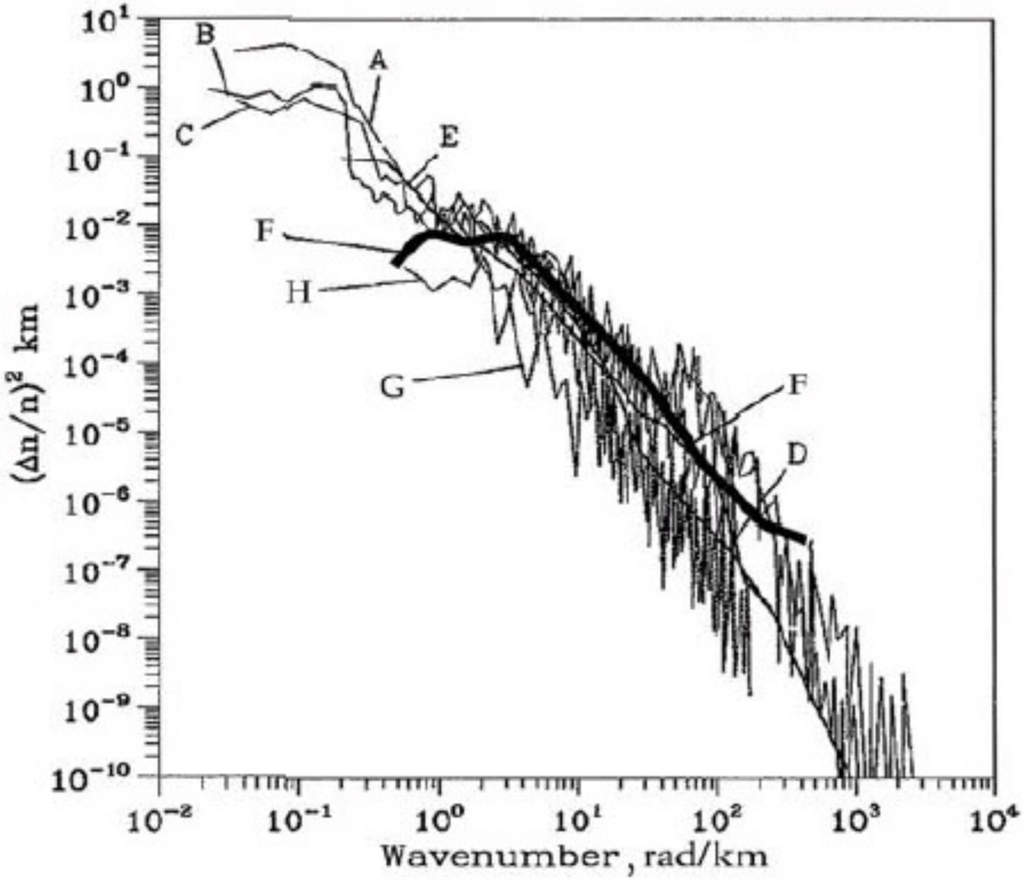

Kelley and Livingston, JGR 2003

'Universal' spectrum
of fluid turbulence

Found in scintillation bubbles,
Barium cloud striations, …

Power law from λ = 100 km
down to λ = 0.01 km

Driving forces at large λ
Cascade through inertial range
Dissipation at short λ

Note: this density spectrum is required for S_4 calculation

Coherent Radar Echoes

from 3 m irregularities

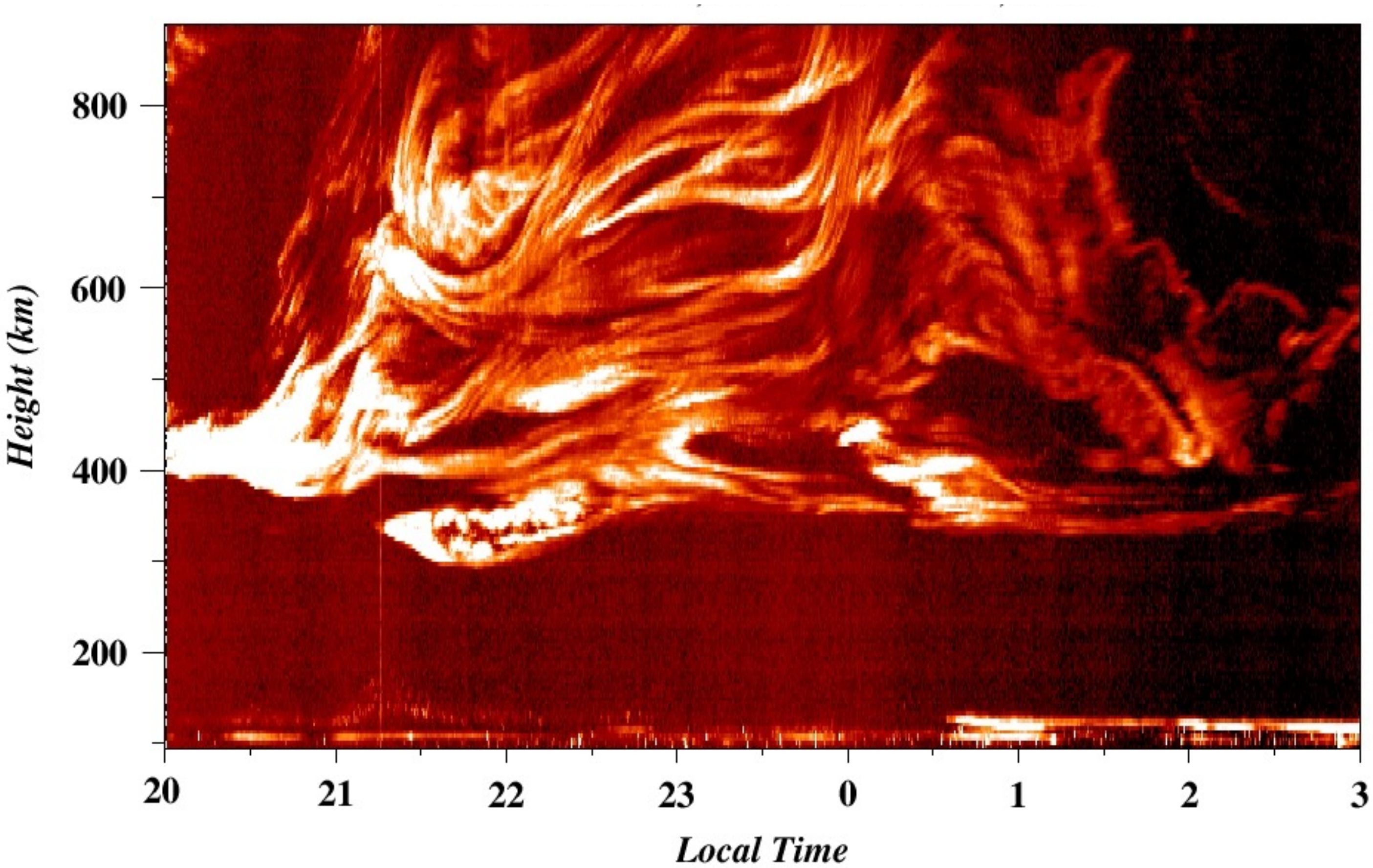

Jicamarca radar view of Ionospheric Disturbance

(Woodman and LaHoz 1976)

Equatorial Ionosphere

Background for Scintillation Phenomena

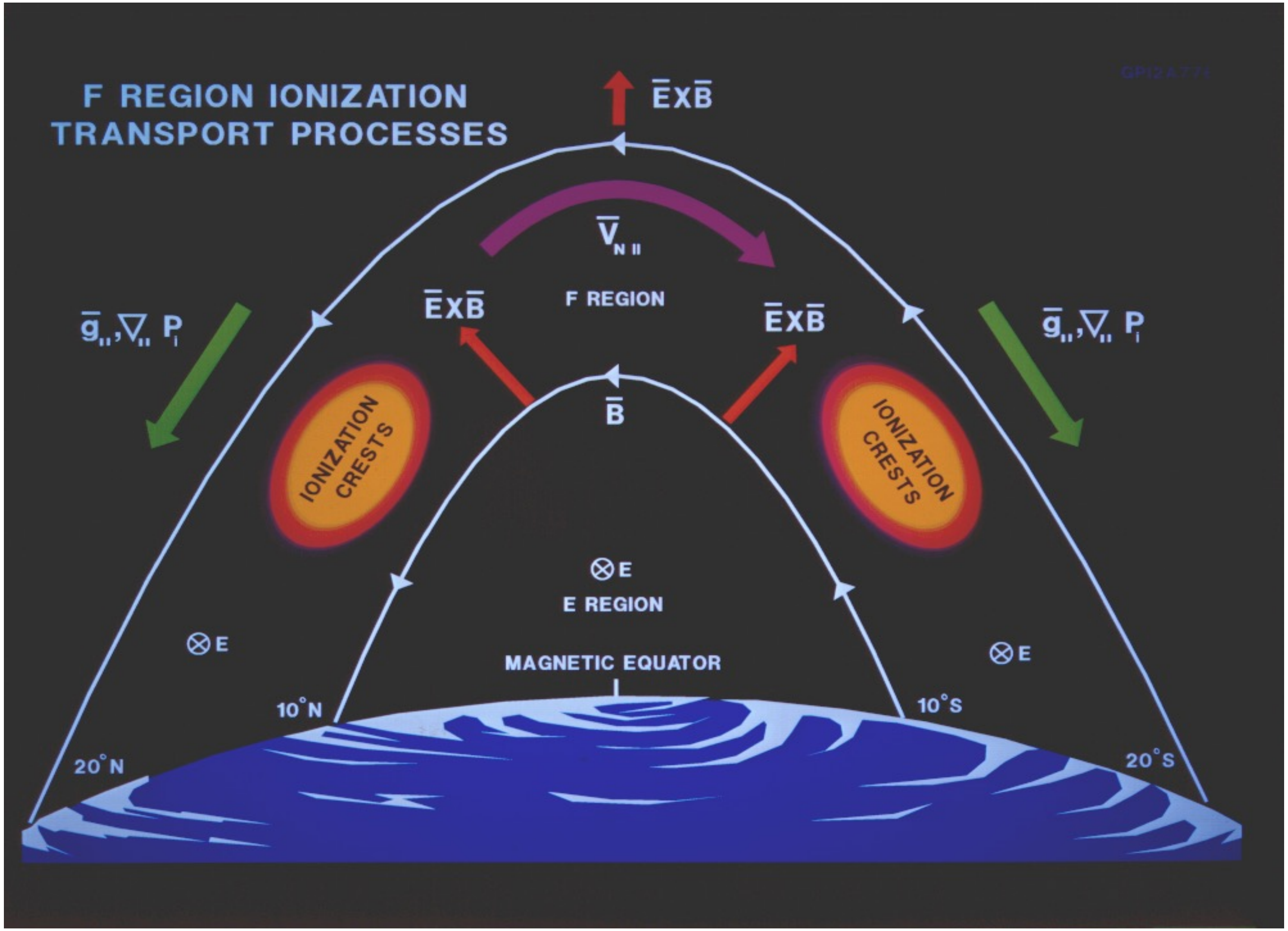

Rayleigh-Taylor Instability

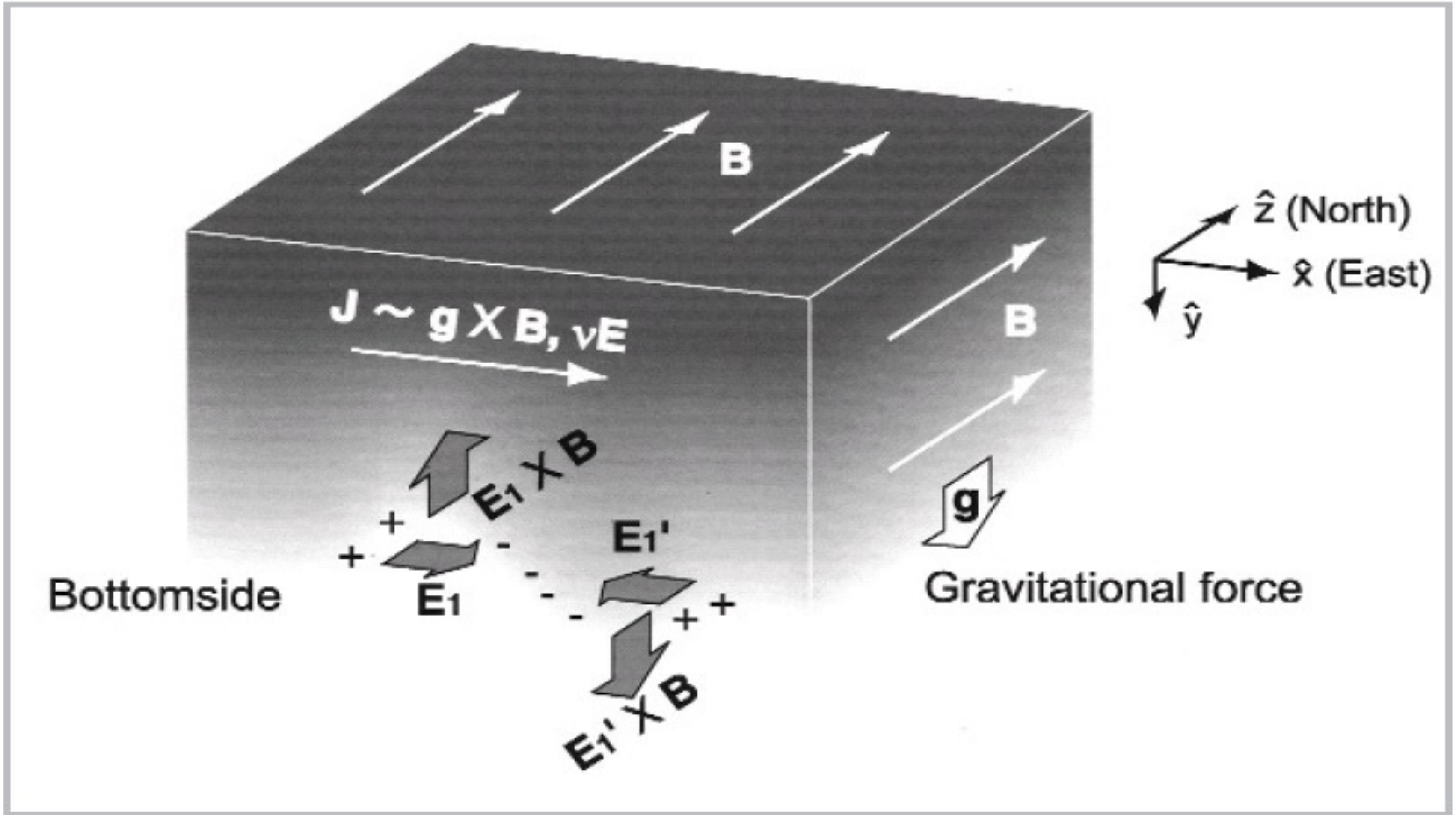

Rayleigh-Taylor Growth Rate

Exponential Growth $A = A_0 e^{\gamma t}$

$$\gamma \approx \frac{\Sigma_F}{\Sigma_F + \Sigma_E}\left[\frac{E \times B}{B^2} + U_n + \frac{g}{\nu^{eff}}\right]\frac{1}{N}\frac{\partial N}{\partial h}$$

- Growth Rate
- Electric Field
- Neutral Wind
- Gravity
- Conductance
- Magnetic Field
- Log Density Gradient

Connections between Plume/Bubble and Ambient Models

- **Ambient: global-scale background**
- **Ambient structure determines whether a region will be unstable**
- **Plume model dependent on ambient parameters of ionosphere**
  - **Neutral density, wind, & temperature**
  - **Plasma density, velocity, & temperature**
- **Ambient models**
  - **Empirical models (Hedin, …)**
  - **Coupled ionosphere/thermosphere models (TIEGCM, CISM, WAM, WACCM-X)**
  - **Data assimilation**
- **Next generation: feedback from plume to ambient**

Sources of Energy

Other regions of MIT system serve as sources of energy for drifts of the low-latitude ionosphere

- Thermosphere
  - Neutral dynamo
  - Both quiet and disturbed times
- Magnetosphere
  - Interplanetary electric field
  - Under/Over shielded by inner magnetosphere
  - Penetration electric fields at low latitudes

Effect of Lower Atmosphere: Neutral-Wind Dynamo

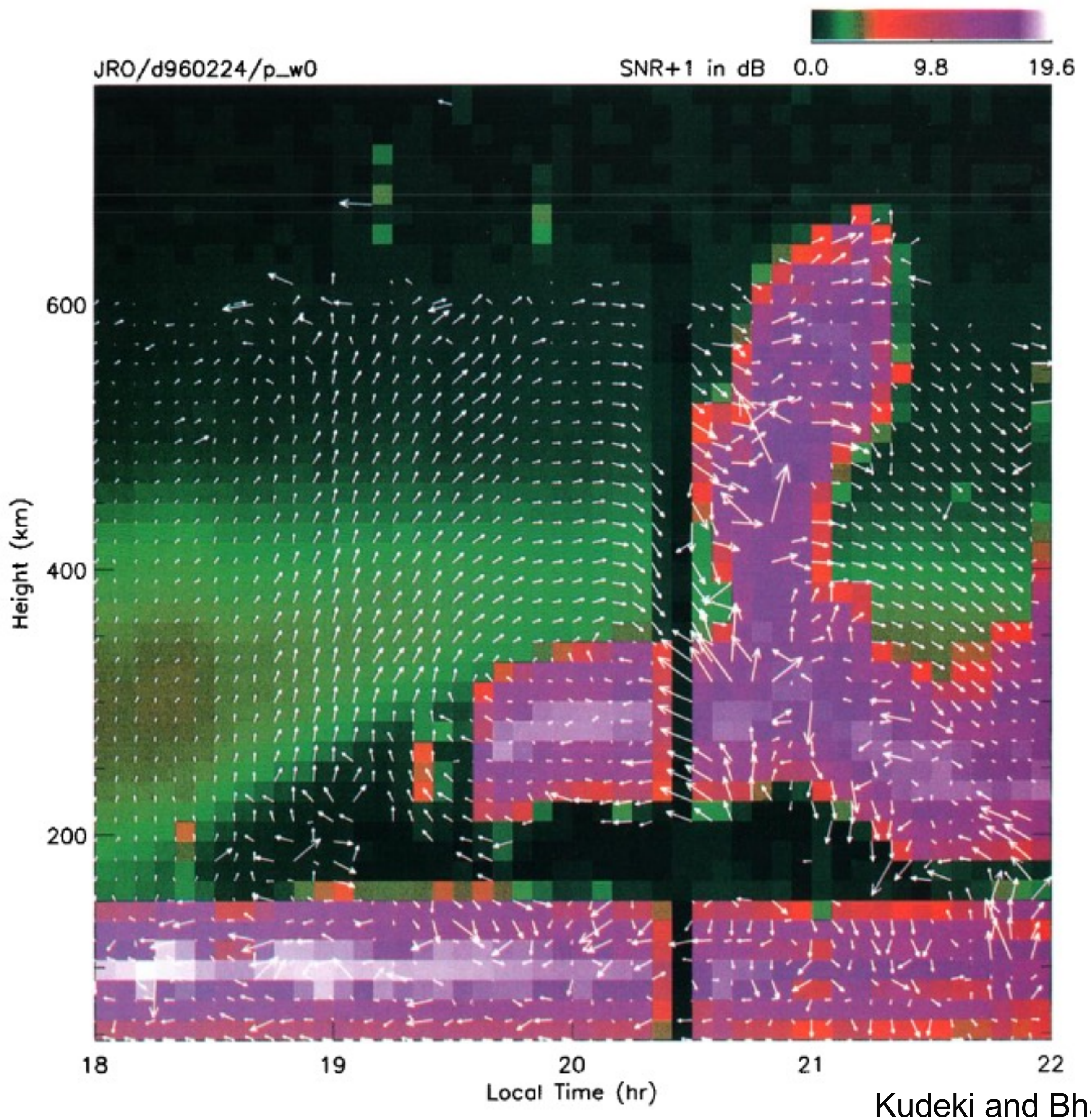

Kudeki and Bhattacharyya 1999

Plasma Drift Velocity and Scintillation

Radar data

Plasma density contours and Strong returns from scintillation

Vert. Plasma velocity

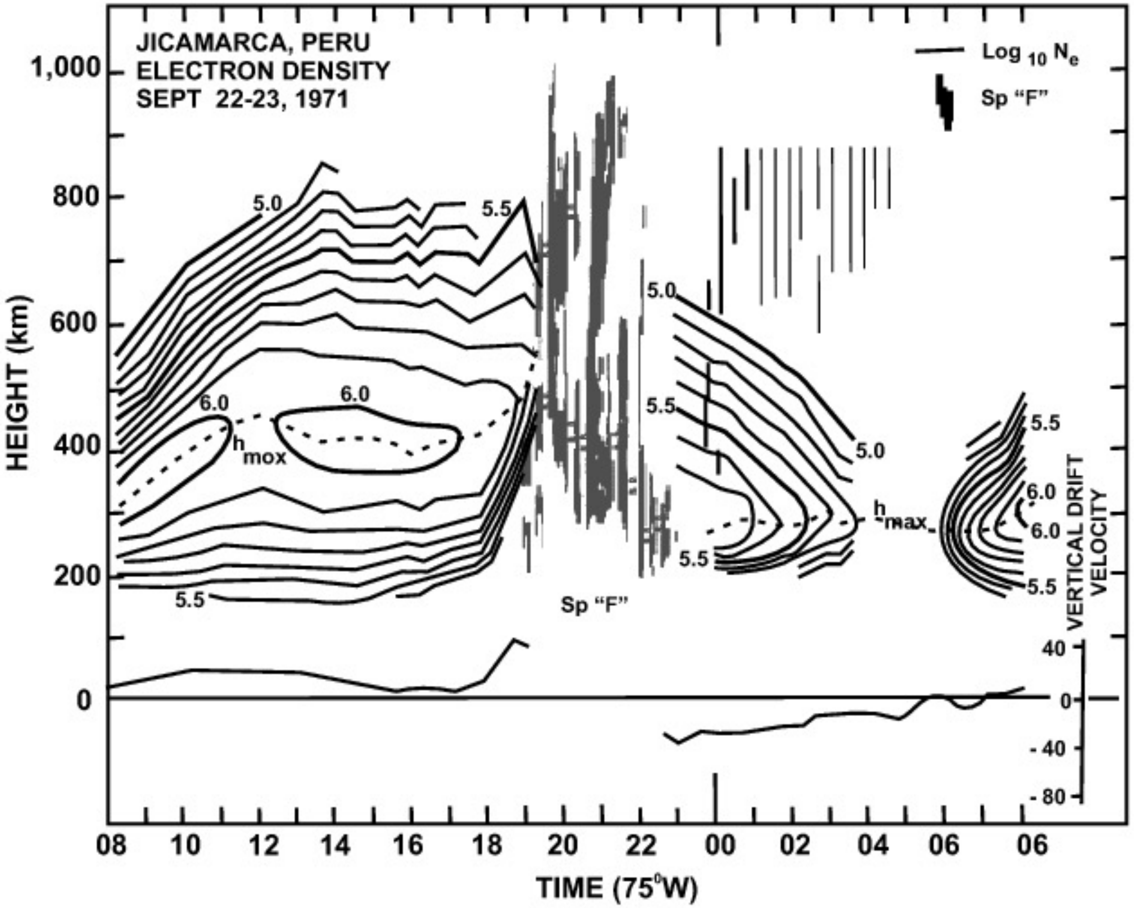

Upward plasma drift at night causes the ionosphere to become more unstable

- **Commonly occurs just after sunset (called pre-reversal enhancement)**
- **Also occurs in early morning hours during geomagnetically active times**

Strength of this drift is most sensitive parameter for scintillation

Effect of Storm-time Penetration Electric Fields

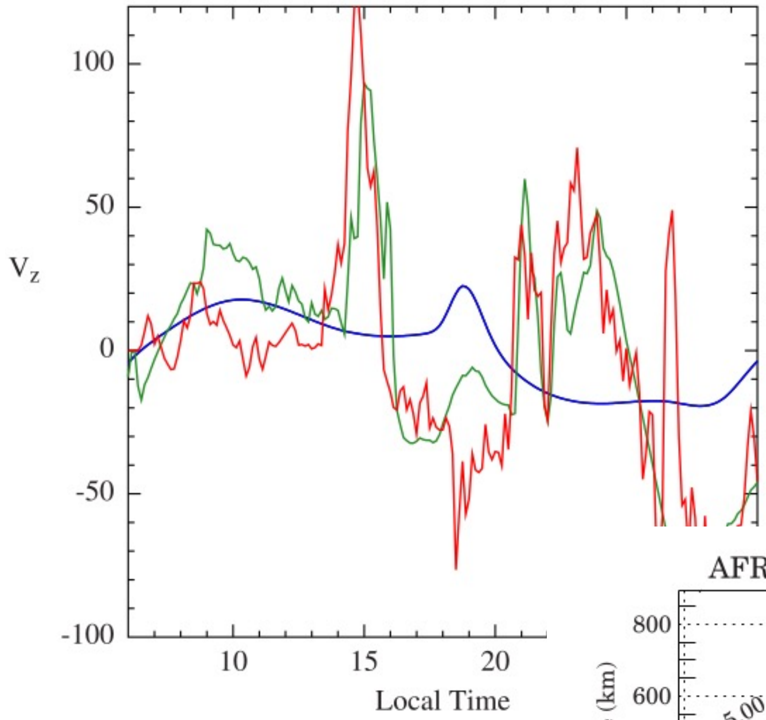

Blue – 'normal' quiet-time vertical drift
Green – drift includes contribution from scaled IMF/SW penetration electric field
Red – observed drift

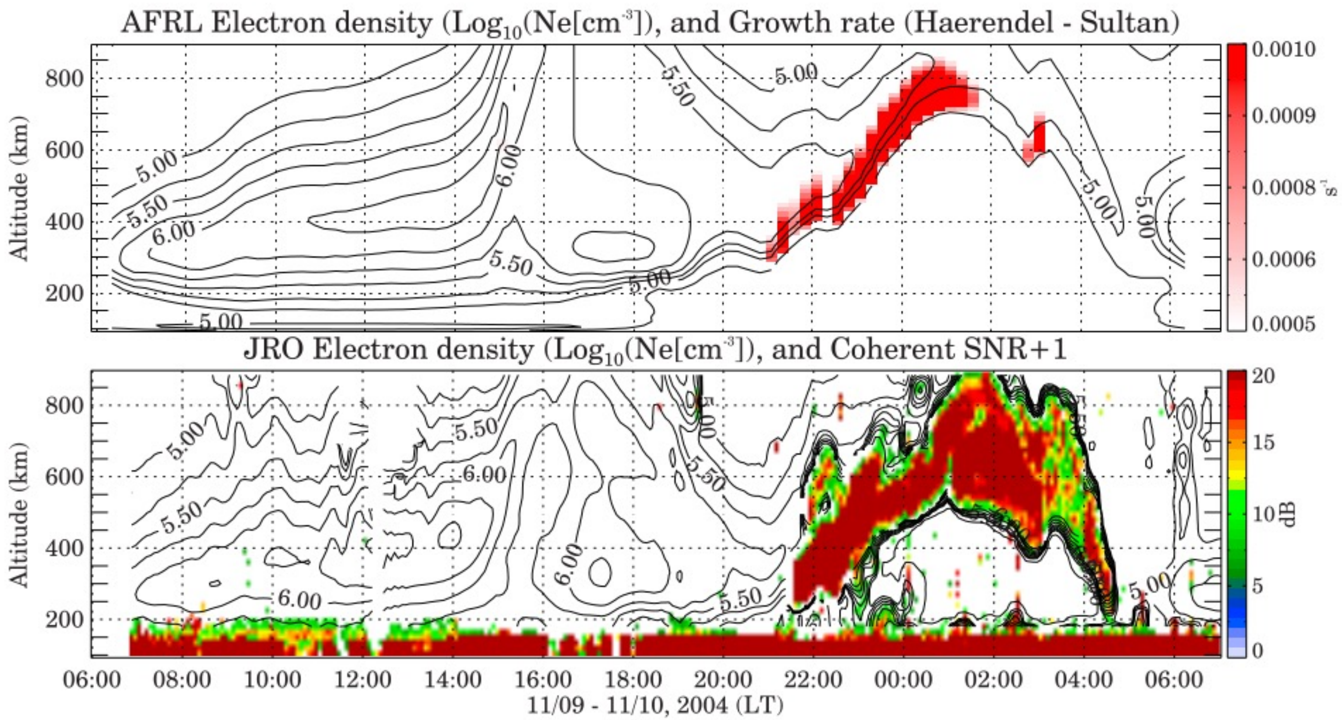

Kelley and Retterer 2008

ESF Plume Models

For radio scintillation estimates, need density around bubble/plume structures

Plume formation through nonlinear evolution of generalized Rayleigh-Taylor instability

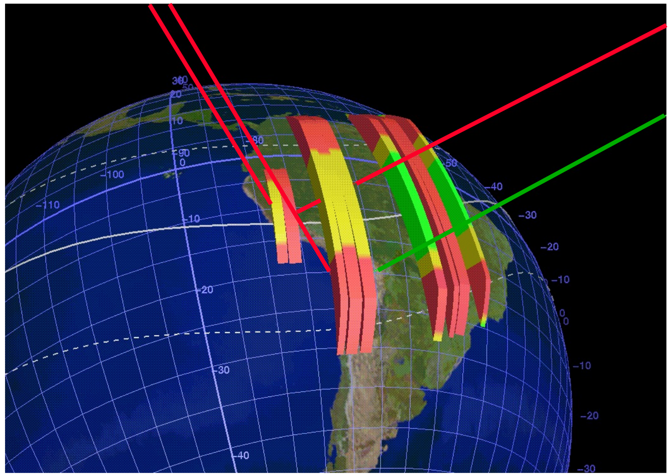

(Figure courtesy of Keith Groves)

Development History – plume models

–Equatorial plane (Ossakow 1976)

–Discrete layers (Zalesak 1982)

–Field-line integrated quantities (Keskinen 1998, Retterer 1999)

–3-D treatment of transport (Retterer 2002; Huba 2008)

–Higher resolution models (Yokoyama 2014)

–3-D treatment of electric fields (Hysell 2022)

Parallel Transport

$$\frac{\partial n}{\partial t} + \nabla_{||} \cdot (n v_{||}) = P - L$$

$$\nu_s v_{||} = \frac{q_s}{m_s} E_{||} + g_{||} - \frac{1}{n_s} \nabla_{||} P_s + \nu_s \mathbf{U}_{||}$$

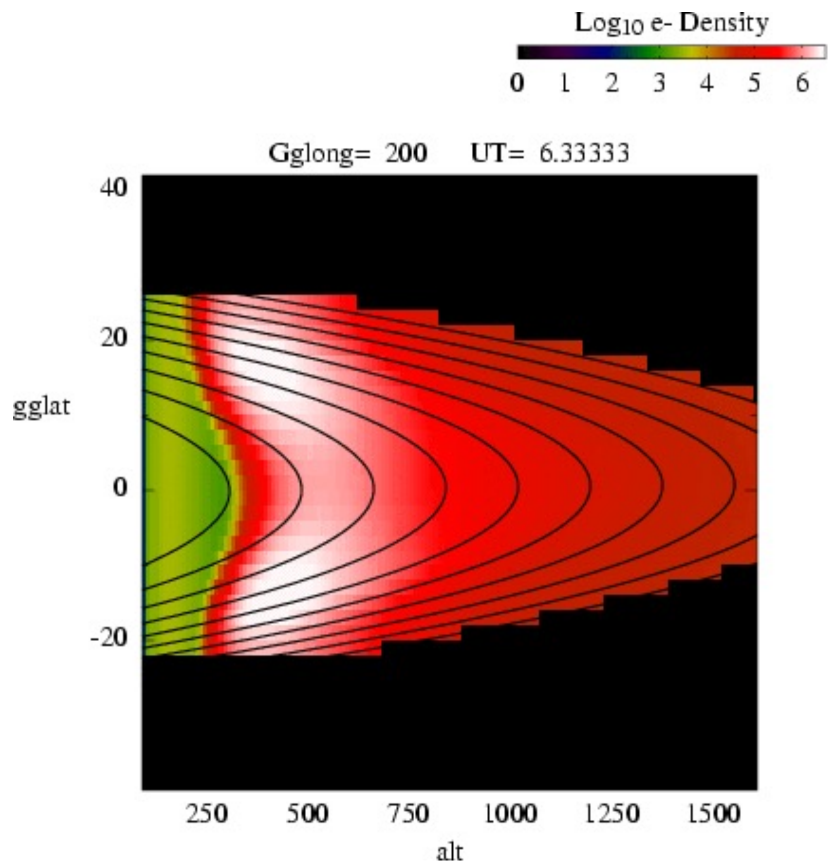

Perpendicular Transport

Continuity Eqn

$$\frac{\partial n}{\partial t} + \nabla_\perp \cdot (n\mathbf{v}_\perp) = 0$$

Momentum Eqn

$$\frac{d\mathbf{v}_s}{dt} = \frac{q_s}{m_s}\mathbf{E} + \mathbf{g} + \Omega_s \mathbf{v}_s \times \hat{\mathbf{B}} - \frac{1}{n_s}\nabla_\perp P_s + \nu_s(\mathbf{U} - \mathbf{v}_s)$$

Inertia-less treatment

$$\mathbf{v_{s\perp}} = k_{1s}\mathbf{A_s} + k_{2s}\mathbf{A_s} \times \hat{\mathbf{B}}$$

Accelerations due to various forces

$$\mathbf{A_s} = \frac{q_s}{m_s}\mathbf{E} + \mathbf{A_{0s}},$$

$$\mathbf{A_{0s}} = \frac{q_s}{m_s}\mathbf{E_0} + \mathbf{g} - \frac{1}{n_s}\nabla_\perp P_s + \nu_s \mathbf{U}$$

Mobilities

$$k_{1s} = \frac{\nu_s}{\nu_s^2 + \Omega_s^2}, \qquad k_{2s} = \frac{\Omega_s}{\nu_s^2 + \Omega_s^2}$$

Electric Fields

Parallel electric field from ambipolar field

Perpendicular fields from current-continuity condition:

No charge build-up implies divergence of current is zero; integrate along field lines:

$$\int \left[\frac{\partial}{\partial \alpha} (j_\alpha h_\beta h_\gamma) + \frac{\partial}{\partial \beta} (h_\alpha j_\beta h_\gamma) \right] d\gamma = 0$$

The coordinate system: We use Euler potentials α and β as orthogonal coordinates that label a field line, while γ denotes position along the field line. α corresponds to the L-shell variable, and β is the longitude (zonal) variable. (h_α h_β h_γ are the metric coefficients for the variables)

Electric Field Calculation

$$\mathbf{j} = nq(\mathbf{v_i} - \mathbf{v_e})$$

$$\Sigma_p = \sum n_i q^2 (k_{1i}/m_i + k_{1e}/\mathbf{M}_e)$$

$$\mathbf{j}_\perp = \Sigma_p \mathbf{E}_\perp + \Sigma_h \mathbf{E}_\perp \times \hat{\beta} + \mathbf{j_0}$$

$$\Sigma_h = \sum n_i q^2 (k_{2i}/m_i + k_{2e}/\mathbf{M}_e)$$

$$\mathbf{j_0} = \sum n_i q \left(k_{1i}\mathbf{A_{0i\perp}} - k_{1e}\mathbf{A_{0e\perp}} + k_{2i}\mathbf{A_{0i\perp}} \times \hat{\beta} - k_{2e}\mathbf{A_{0e\perp}} \times \hat{\beta} \right)$$

$$\mathbf{E}_\perp = -\frac{\hat{\alpha}}{h_\alpha}\frac{\partial \Phi}{\partial \alpha} - \frac{\hat{\beta}}{h_\beta}\frac{\partial \Phi}{\partial \beta}$$

$$\frac{\partial}{\partial \alpha}\left(\Sigma_{p\alpha}\frac{\partial \Phi}{\partial \alpha} + \Sigma_{h\alpha}\frac{\partial \Phi}{\partial \beta}\right) + \frac{\partial}{\partial \beta}\left(\Sigma_{p\beta}\frac{\partial \Phi}{\partial \beta} - \Sigma_{h\beta}\frac{\partial \Phi}{\partial \alpha}\right) = \frac{\partial j_{0\alpha}}{\partial \alpha} + \frac{\partial j_{0\beta}}{\partial \beta}$$

$$\Sigma_{p\alpha} = \int \frac{\Sigma_p}{{h_\alpha}^2} h_\alpha h_\beta h_\gamma d\gamma, \qquad \Sigma_{p\beta} = \int \frac{\Sigma_p}{{h_\beta}^2} h_\alpha h_\beta h_\gamma d\gamma$$

$$j_{0\alpha} = \int \frac{j_{0\alpha}}{h_\alpha} h_\alpha h_\beta h_\gamma d\gamma,$$

$$j_{0\beta} = \int \frac{j_{0\beta}}{h_\beta} h_\alpha h_\beta h_\gamma d\gamma$$

$$\Sigma_{h\alpha} = \Sigma_{h\beta} = \int \frac{\Sigma_h}{h_\alpha h_\beta} h_\alpha h_\beta h_\gamma d\gamma$$

3-D Bubbles

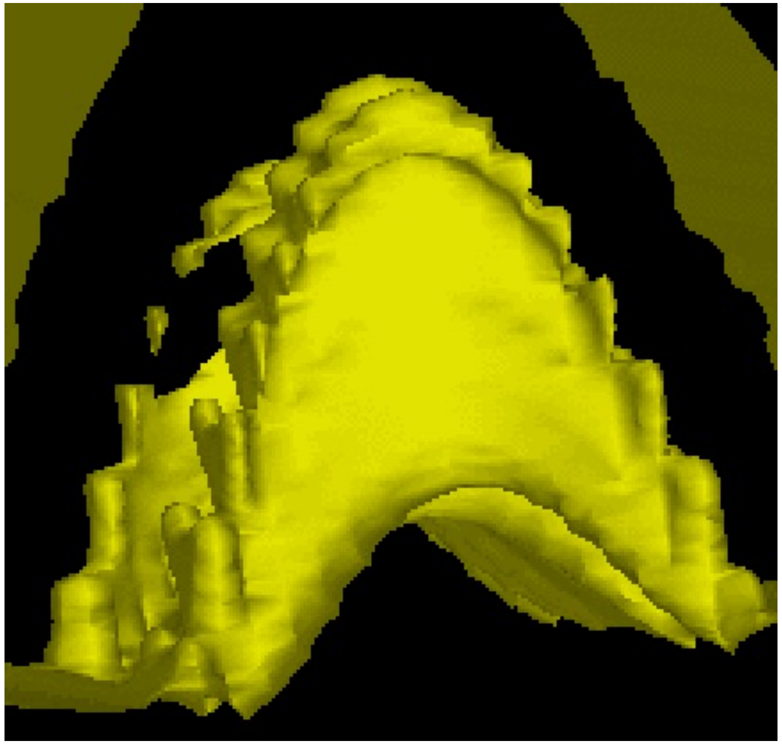

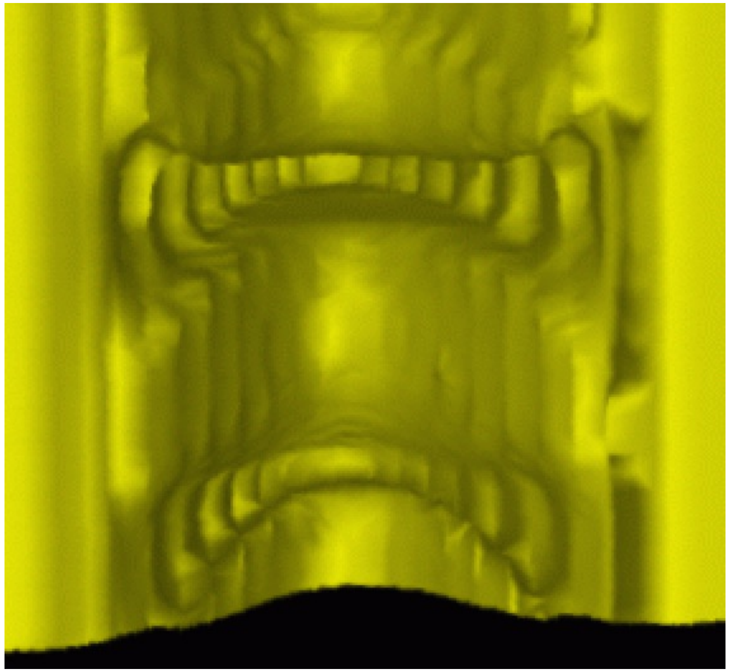

- Isodensity surfaces (density= 10^5 cm-3); snapshots of structure at one instant of time
- The left figure looks from the West, horizontally, showing the bubble more or less following the geomagnetic field line north to south
- The figure on the right is looking up from below the bubble, again showing the north/south orientation of the bubble

Plume Evolution

isodensity surface   10^5 cm-3

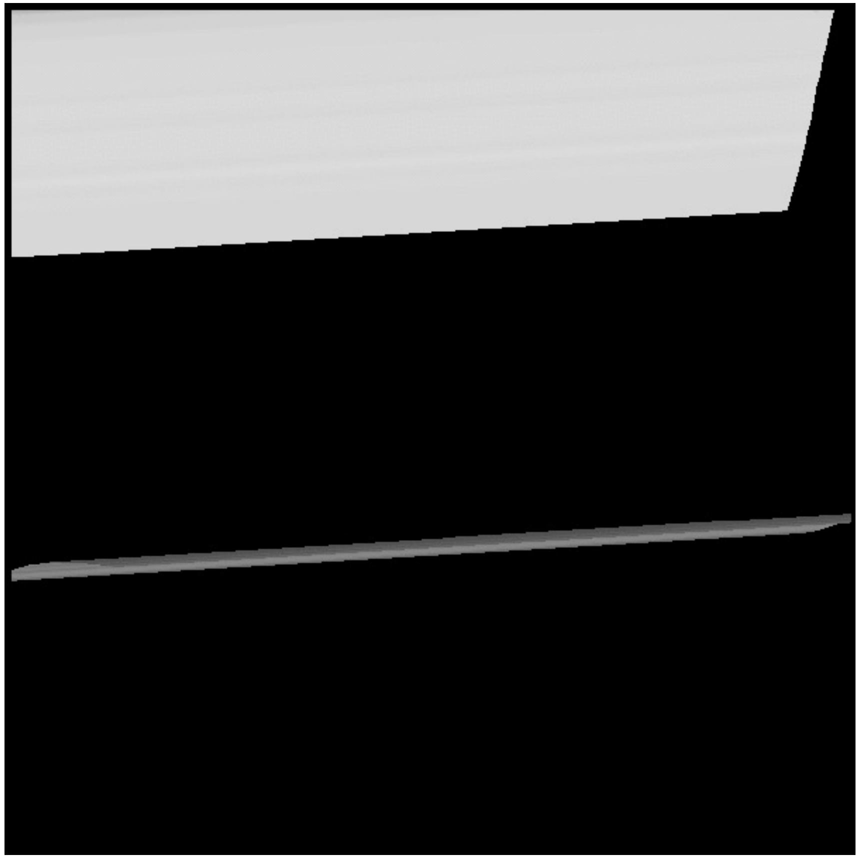

3-D Bubbles

near Appleton Anomaly

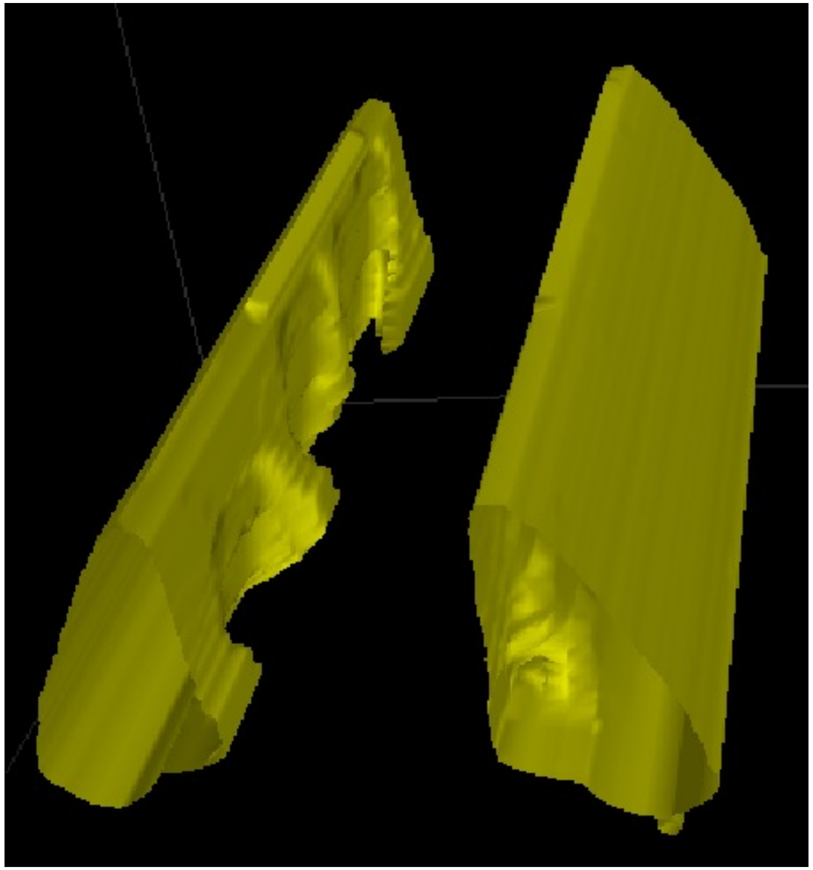

- Isodensity surfaces (density= 10^6 cm-3); snapshot of structure at one instant of time
- This higher density reveals the structure around the Appleton anomalies
- Note that the inside (lower latitude edge) shows structuring with the bubbles, but the outside does not.

Density in Equatorial Plane

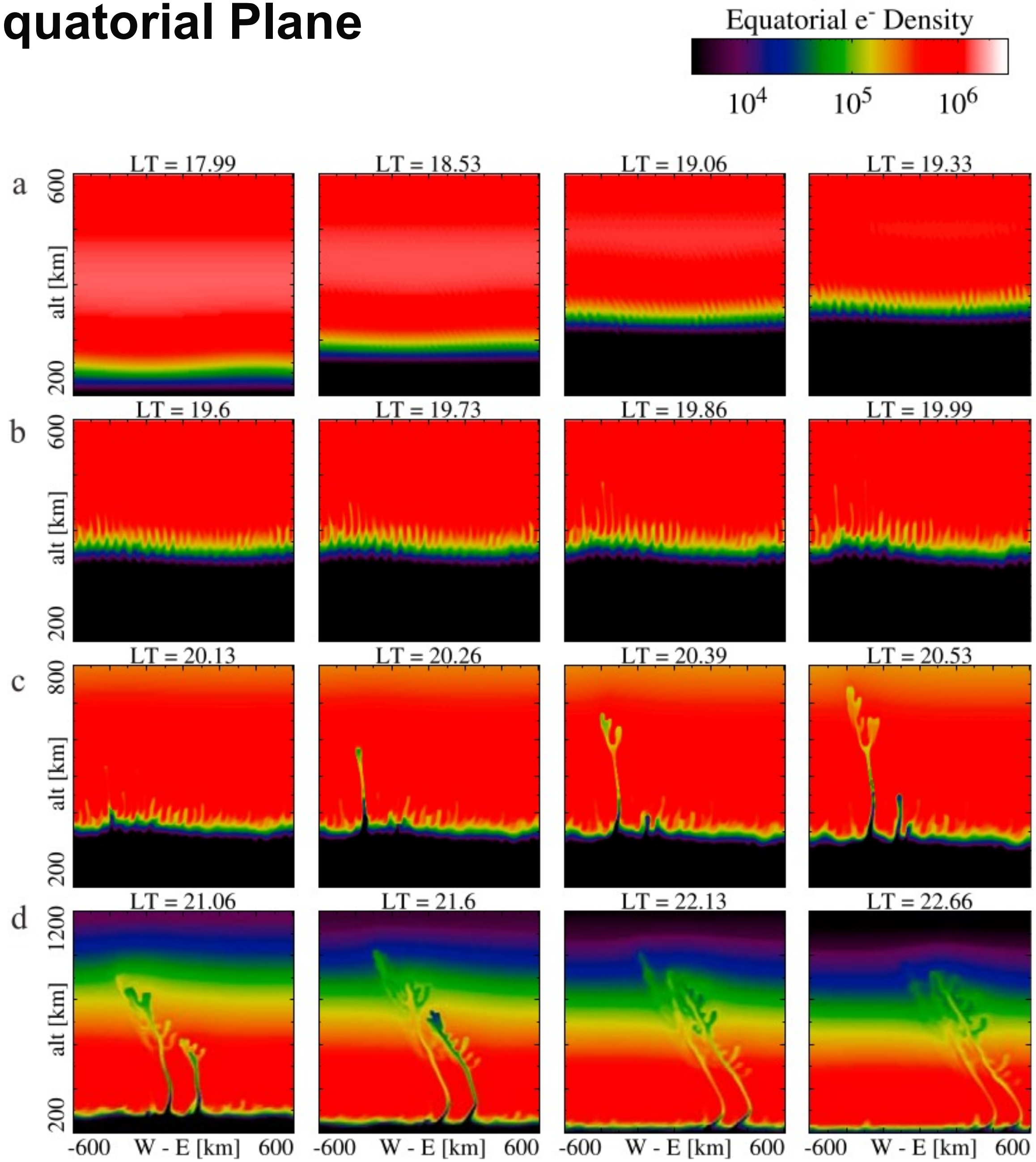

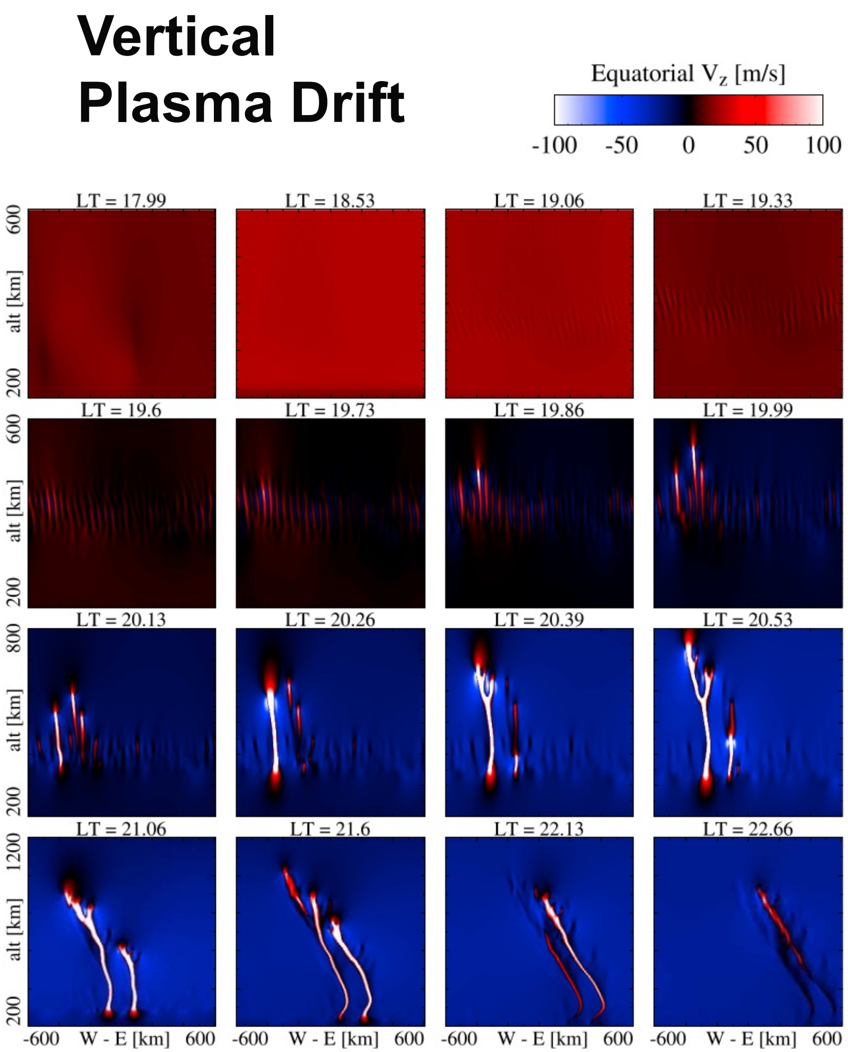
Vertical Plasma Drift
Equatorial V_z [m/s]
-100 -50 0 50 100
LT = 17.99
LT = 18.53
LT = 19.06
LT = 19.33
LT = 19.6
LT = 19.73
LT = 19.86
LT = 19.99
LT = 20.13
LT = 20.26
LT = 20.39
LT = 20.53
LT = 21.06
LT = 21.6
LT = 22.13
LT = 22.66
alt [km]
200
600
800
1200
-600 W - E [km] 600

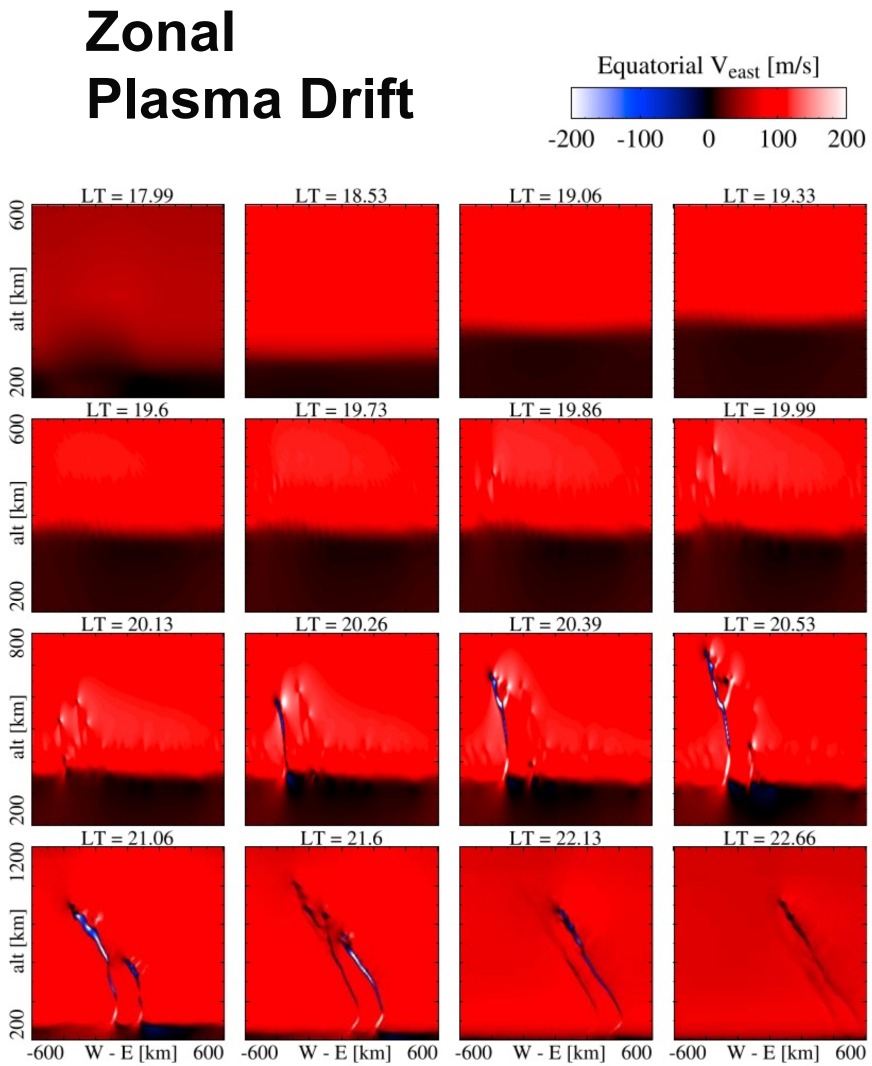
Zonal Plasma Drift
Equatorial V_{east} [m/s]
-200 -100 0 100 200
LT = 17.99
LT = 18.53
LT = 19.06
LT = 19.33
LT = 19.6
LT = 19.73
LT = 19.86
LT = 19.99
LT = 20.13
LT = 20.26
LT = 20.39
LT = 20.53
LT = 21.06
LT = 21.6
LT = 22.13
LT = 22.66
alt [km]
200
600
800
1200
-600 W - E [km] 600

Density and Vert Drift in Eq Plane

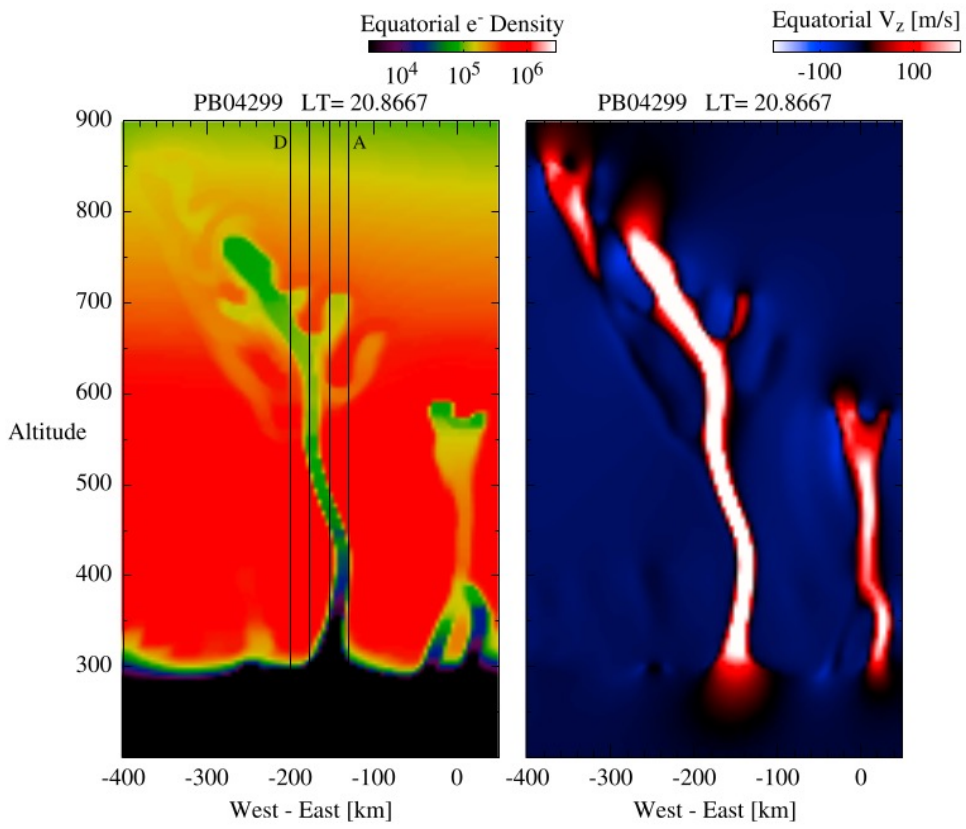

Density in Mag-Field Plane

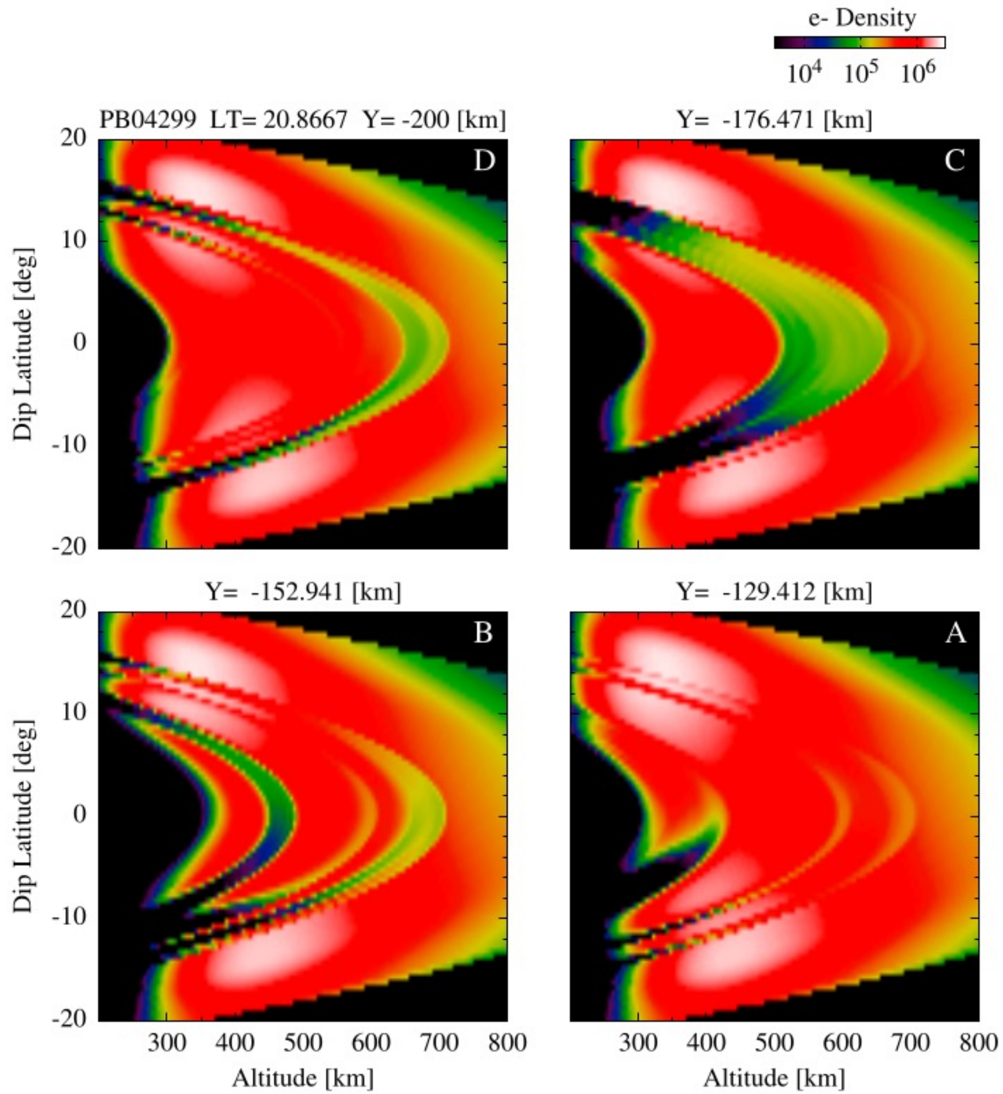

Bubble Structure in Airglow

1356 A emission, Nadir scan geometry
GUVI instrument on TIMED satellite
(Paxton et al.)

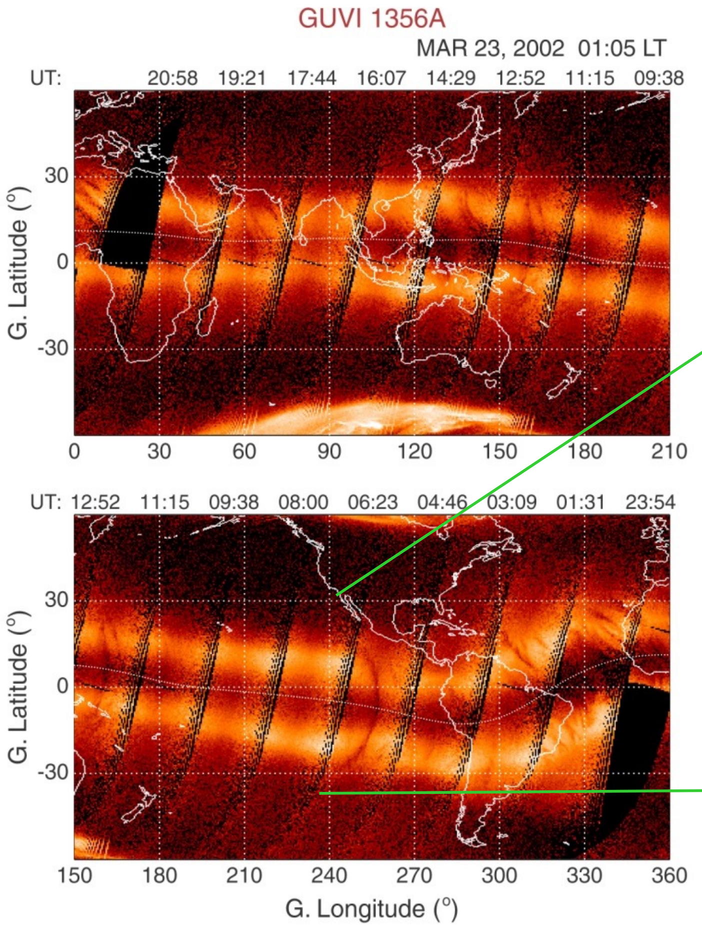

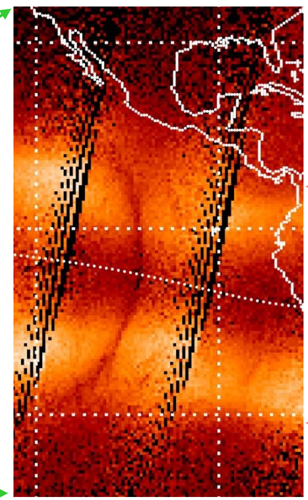

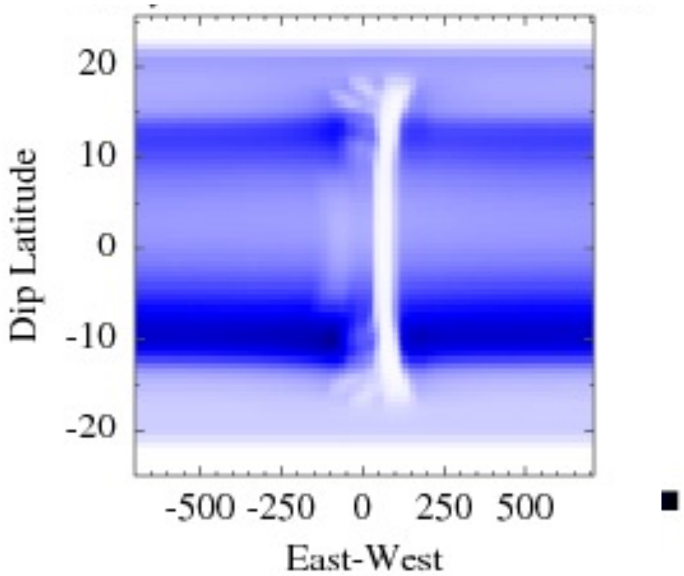

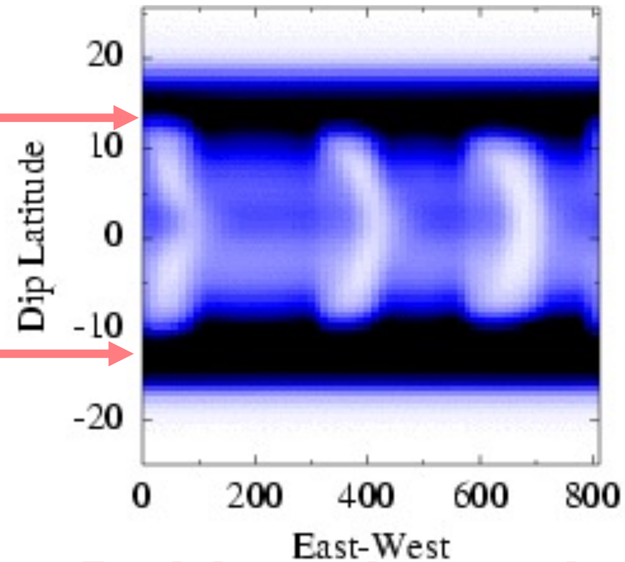

Bubble simulations

GOLD Satellite Observations

Airglow Depletions Seen from Geostationary Height

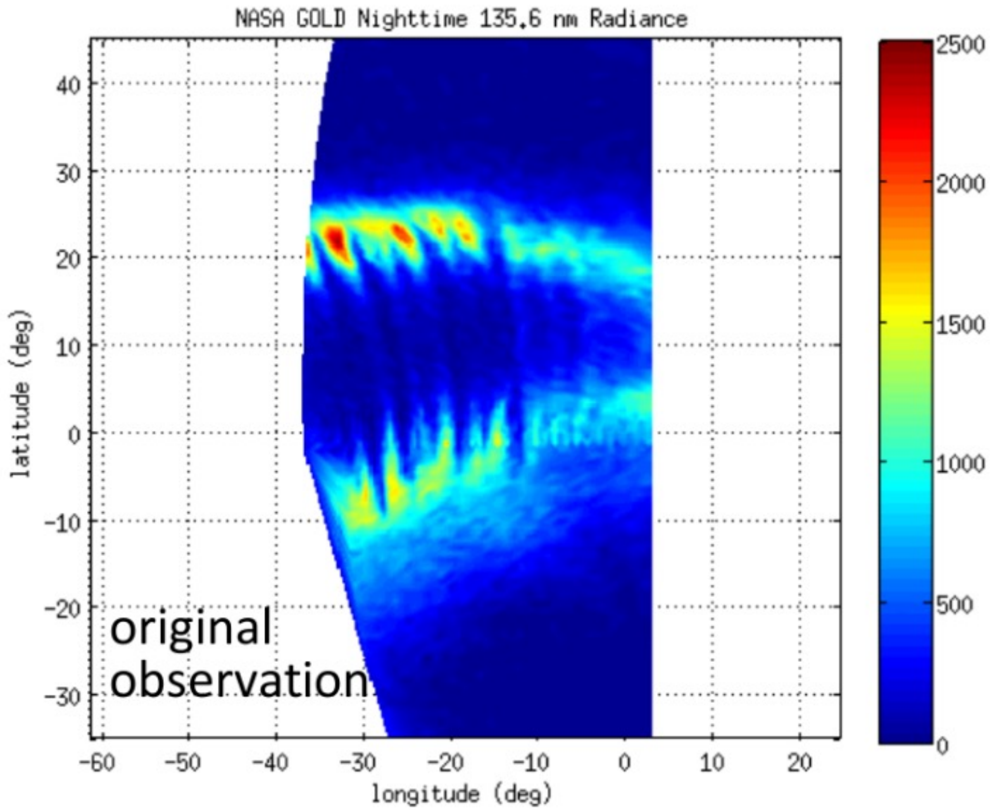

Spacing of Fully Formed Plumes gives a hint of original perturbation structure

Rezy Pradipta

Initial Conditions

Gravity-Wave Seeding

Sometimes the initial perturbation is not so small

Event observed by AE-E satellite:

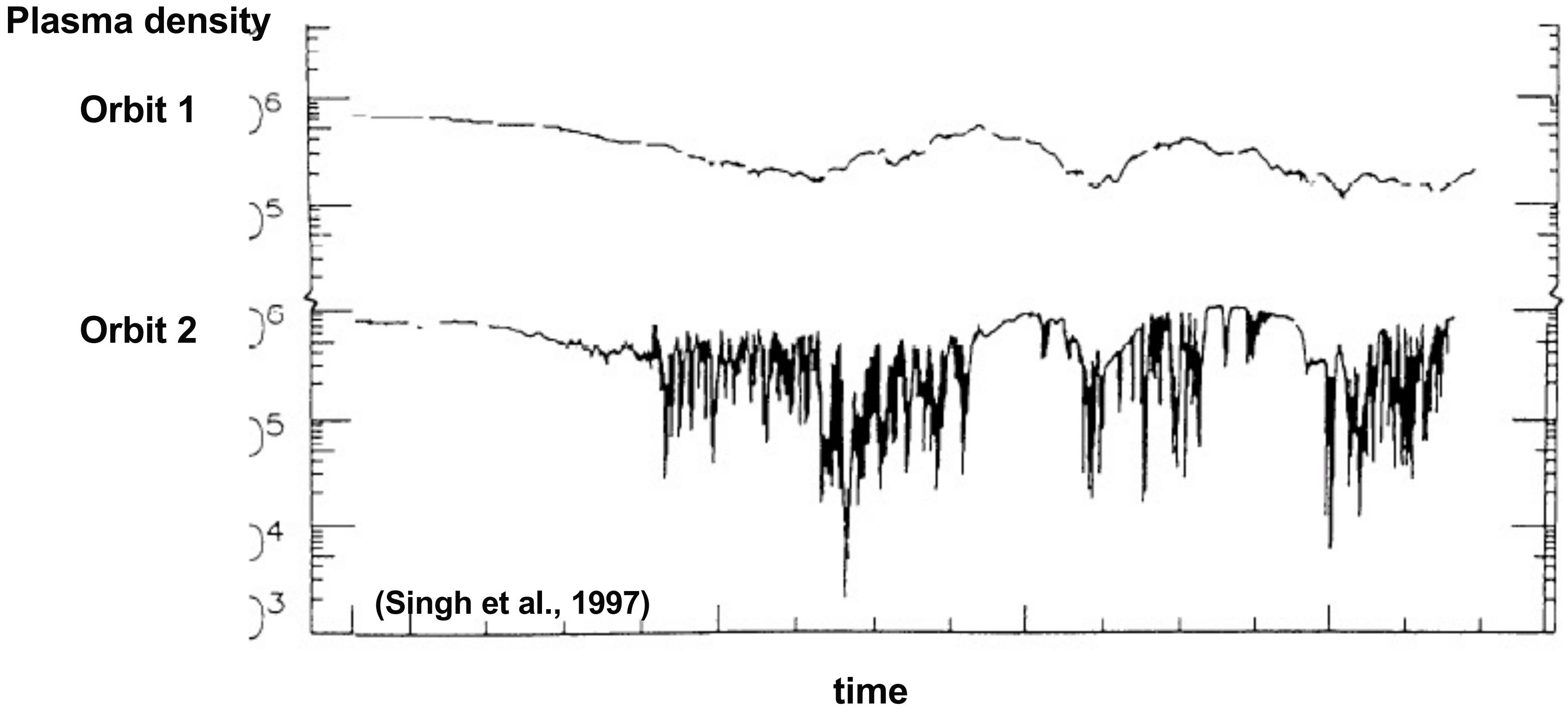

Scintillation Forecasting

Butterfly Problem

- **Plumes develop nonlinearly out of small (unobservable) perturbations**
- **Because of the lack of detailed enough data on these perturbations, it would be impossible to attempt to simulate individual bubbles/plumes or the temporal sequence of radio fades accurately in detail**
- **Instead, we aim to estimate statistical properties of density irregularities (spectrum) to help estimate statistical properties of scintillation (expected level of signal-strength fluctuations)**

Scintillation Strength Theory

S_4 is a measure of Signal-Strength Scintillation:

RMS of Intensity fluctuations / Average signal Intensity

S_4 ranges from 0 to 1 (S_4 = 0.6 corresponds to signal fades of 10 dB)

Observation Geometry:

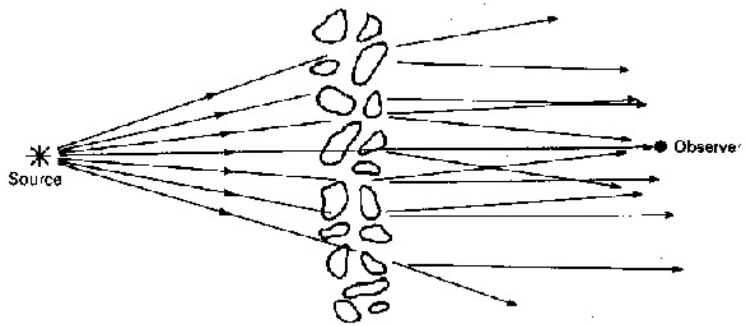

Local phase delay dependent on plasma density:

$$\frac{c^2k^2}{\omega^2} = 1 - \frac{\omega_p^2}{\omega^2}$$

Density irregularities lead to scattering

Use diffraction theory for weak scattering

Scintillation Strength

Phase-Screen formula

- Analytical formula for S4, the statistic for signal-intensity scintillations (Costa and Kelley, 1977)
- S4 expressed in terms of an integral over power-spectral density of plasma density (*n*) integrated along signal path
- Thin phase-screen, weak scattering approximation
- Extend application with saturation formula determined from comparisons with full-wave calculations

$$S_4^2 = 4(r_e\lambda)^2 \int \frac{dk_t}{2\pi} \quad \sin^2\left[\frac{k_t^2}{k_f^2}\right] \quad \frac{|n(k_t, k_s = 0)|^2}{L_t}$$

where

$$k_f^2 = \frac{4\pi}{\lambda h_s}$$

Fresnel wavelength:
500 m at 250 MHz
250 m at 1000 MHz

$$n(k_t, k_s = 0) = \int ds\; dt\; n(s,t)\; e^{ik_t t} = \int dt\; e^{ik_t t} \int ds\; n(s,t)$$

Simulation Irregularity Spectra

Density Power Spectra

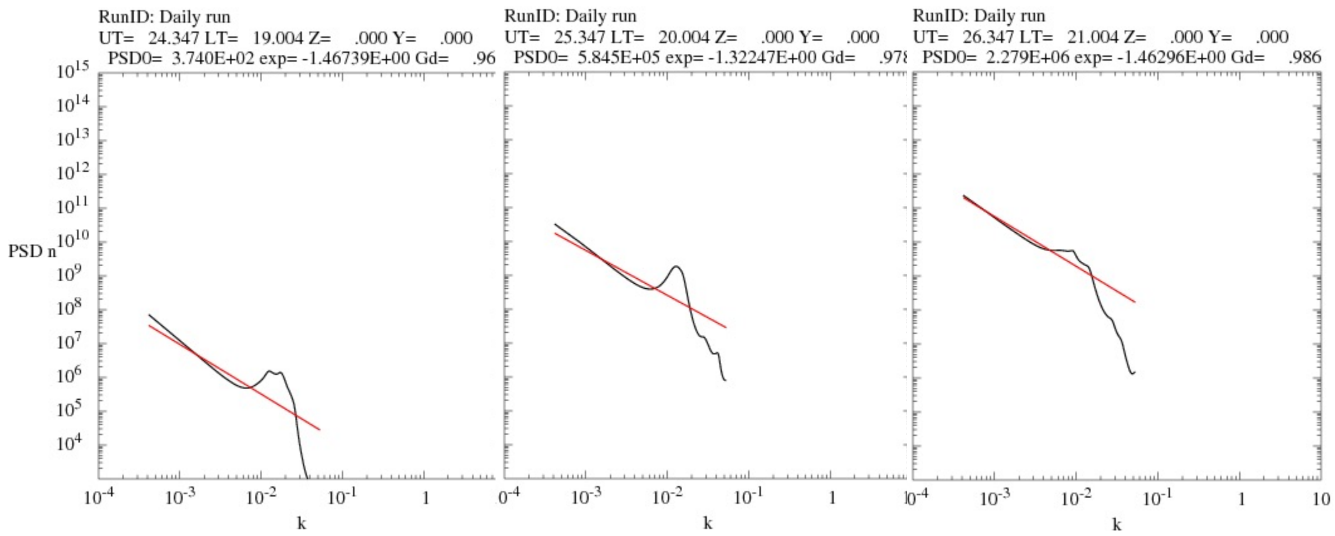

Spectral Characteristics

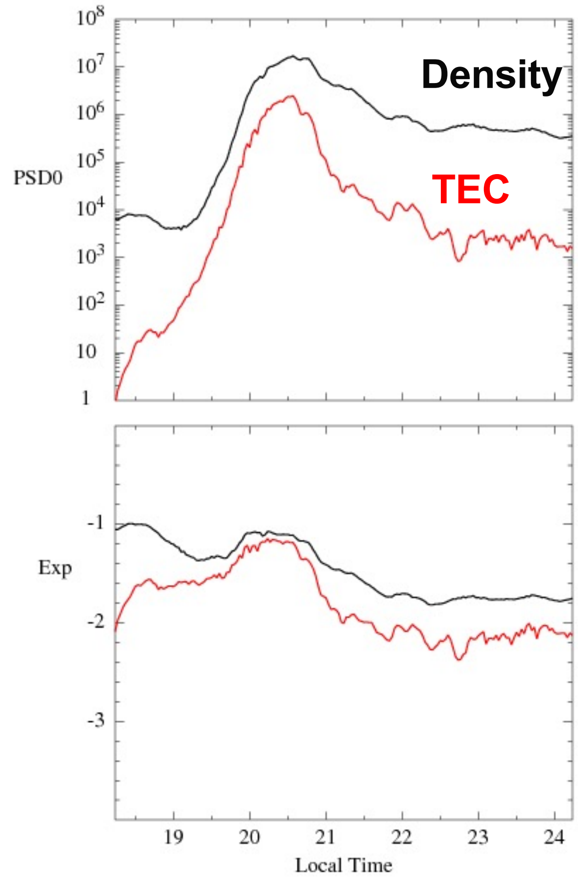

Spectra of density irregularities at 19, 20, 21 hours LT as a function of East-West wavevector *(1/km)*

Red lines: power laws (fitted to long wavelengths, least affected by grid numerics)

Characteristics: power-law amplitude and spectral index

Scintillation Strength

Latitude/local time map for one plume

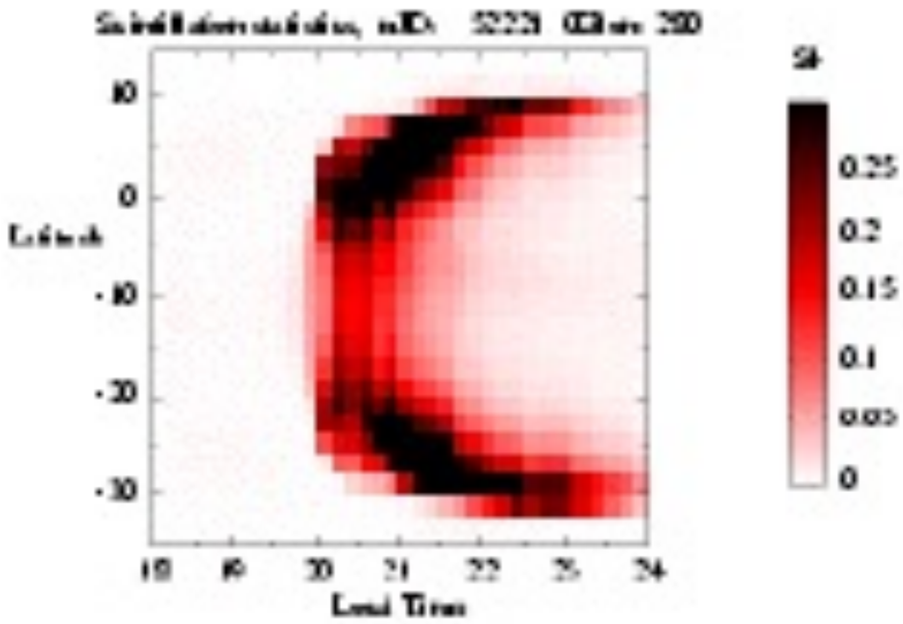

S4 scintillation strength at 250 MHz vertical incidence for an evening in South American sector, using model driven by ionosonde plasma velocity data

Note rapid spread in latitude as bubbles rise; the peaks in scintillation near the peaks in density at the equatorial anomalies

Comparison with SCINDA Observations

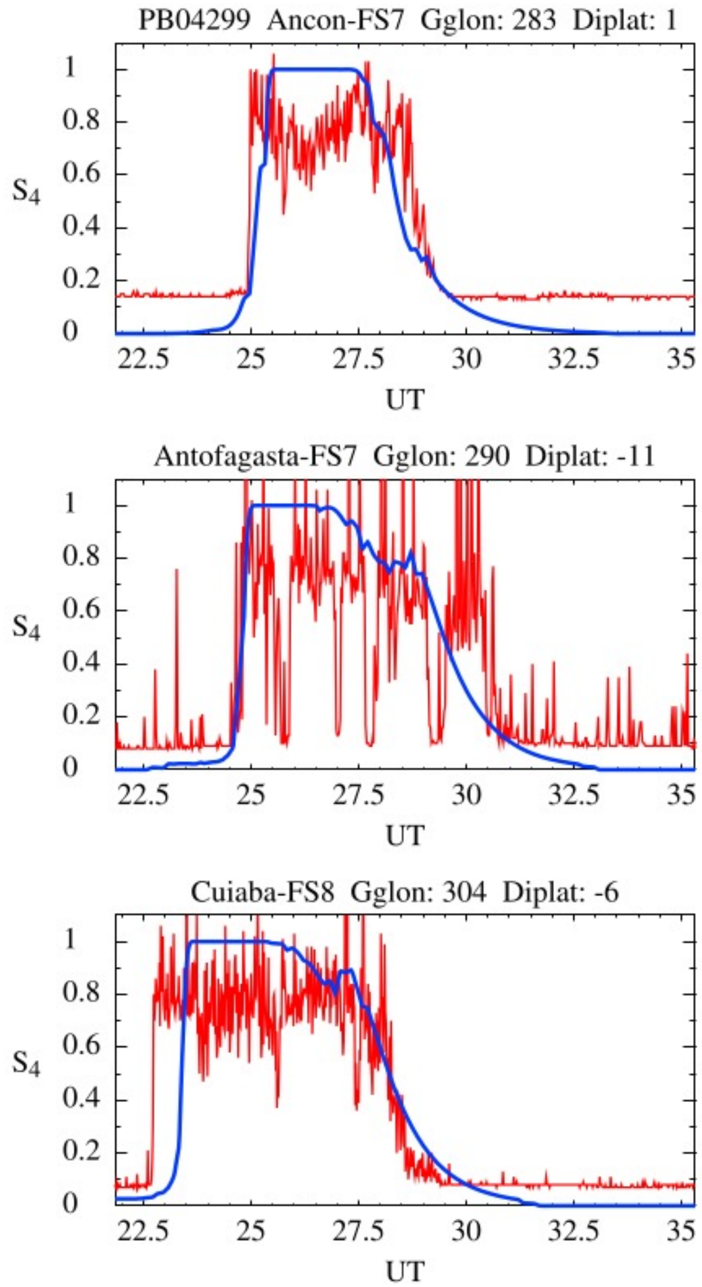

Scintillation Strength

Global Grid

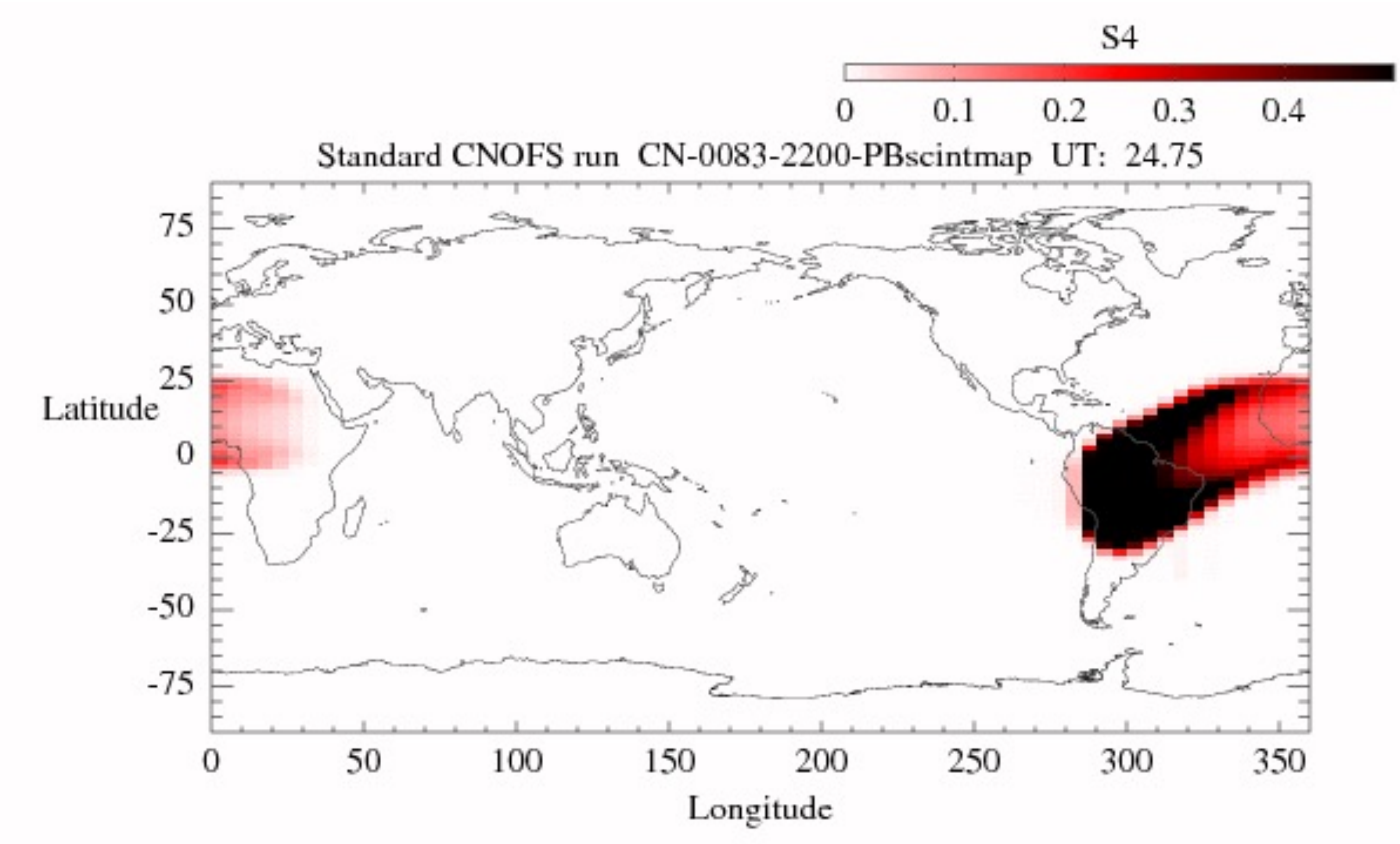

Merge scintillation produced by different plumes at many locations and times into a temporal series of global maps

PBMOD at CCMC: daily run

Scintillation and Bubble Climatology

DMSP plasma-depletion frequency
(1989 – 2002 data)

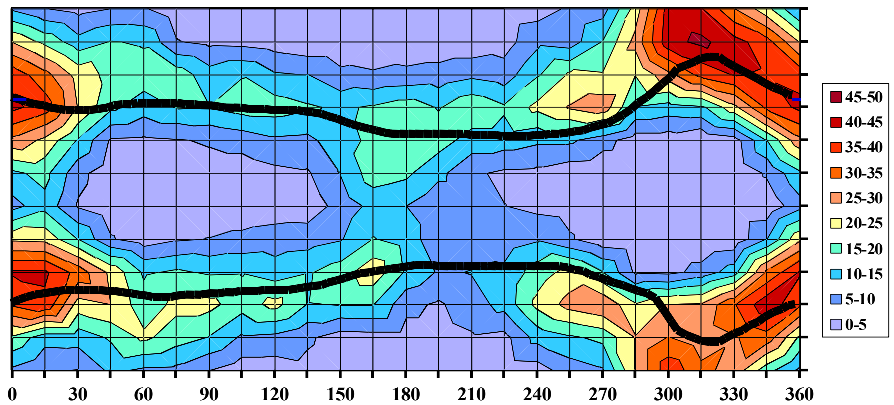

(Burke et al, 2004)

PBMOD S4 Estimation

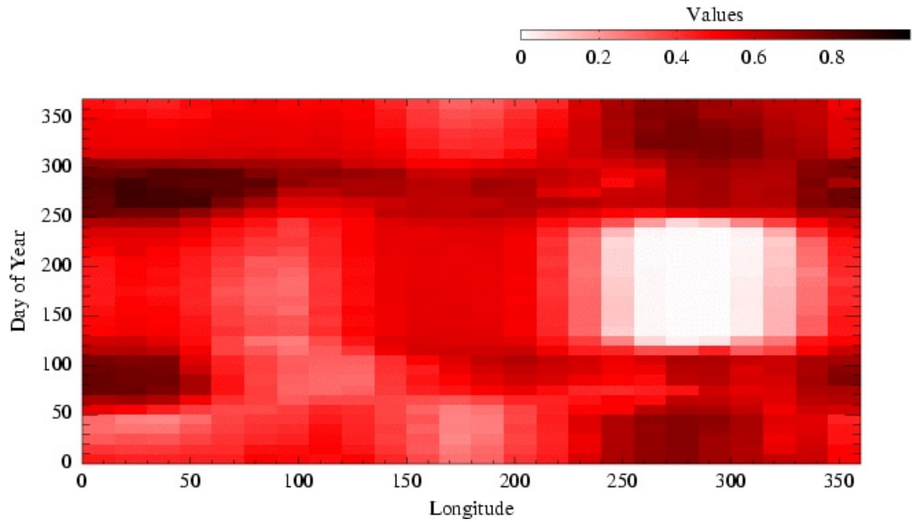

Occurrence of scintillation predicted by PBMOD model matches observed frequency as a function of longitude and day of year Similar patterns established by Aarons (BU) for scintillation

Bubble Climatology

Solar-Cycle Variation

Plasma Density Model and RT growth rate

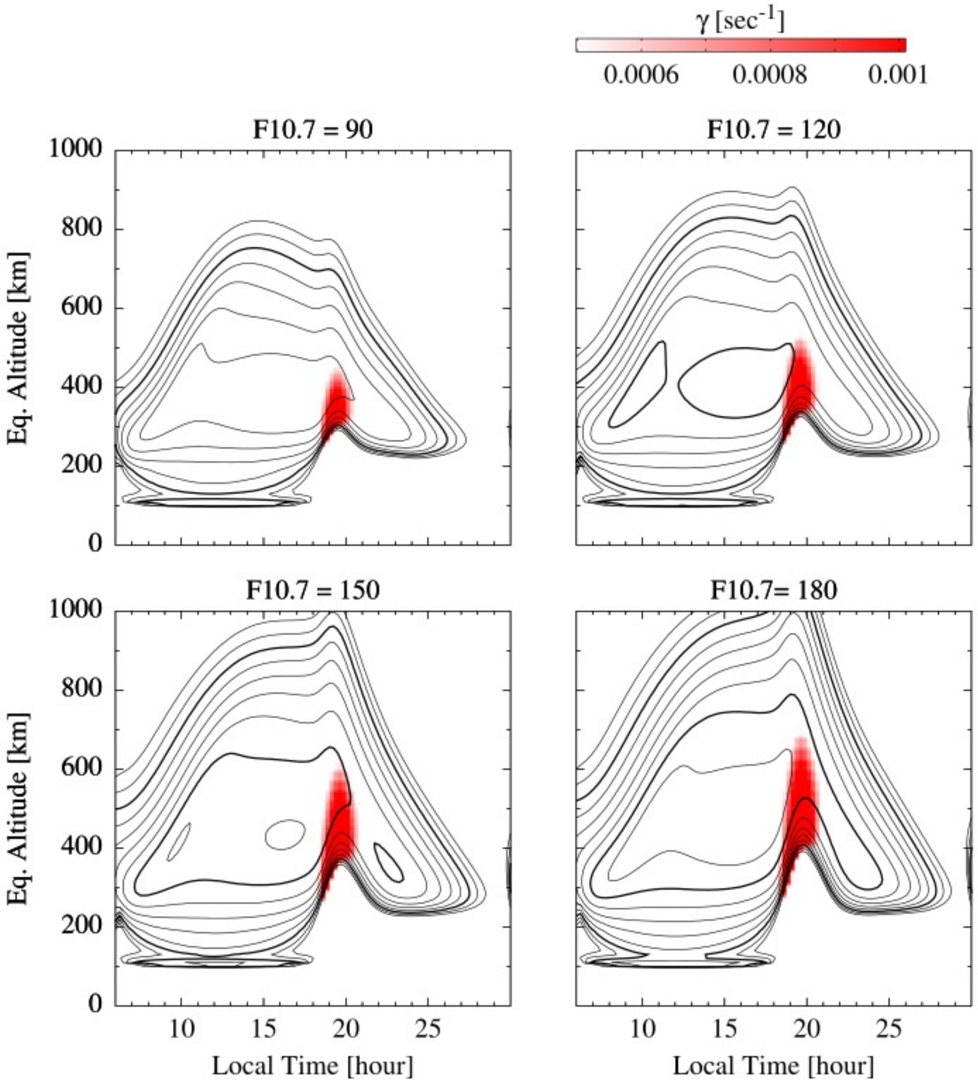

Contours: model plasma density
Red fill: region of RT instability

Bubble Climatology

Solar-Cycle Variation

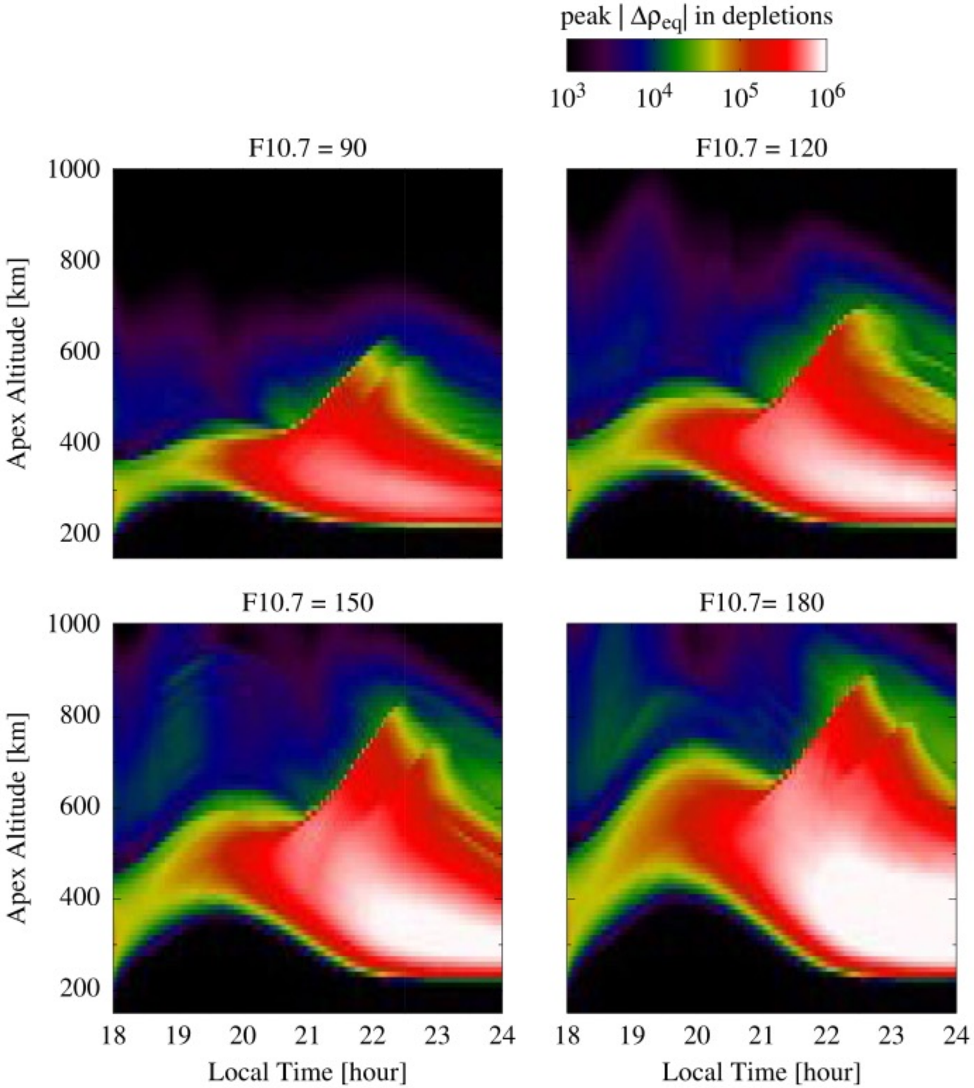

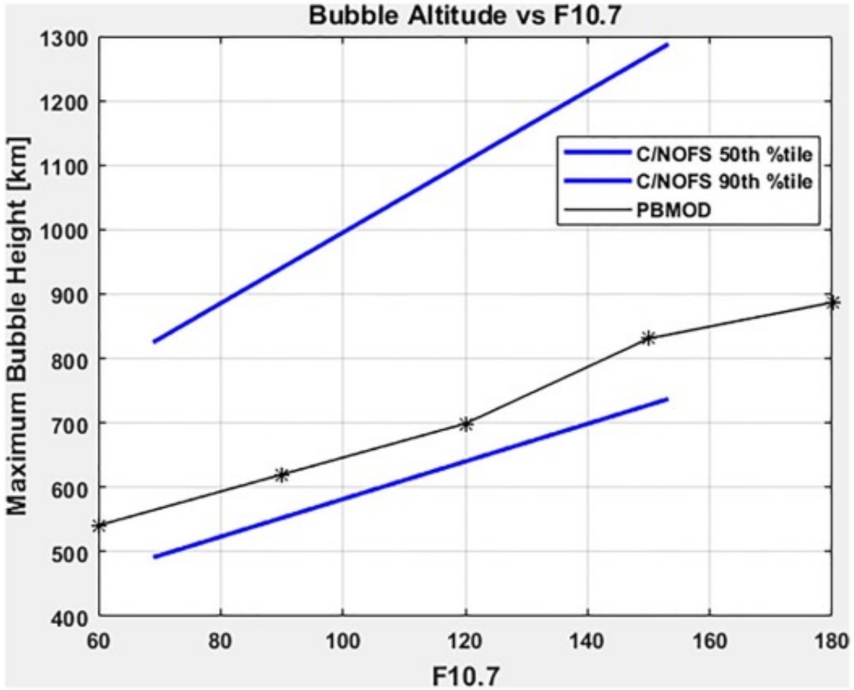

Joshi et al., 2022

Post-Midnight Irregularities over Africa

C/NOFS Observations

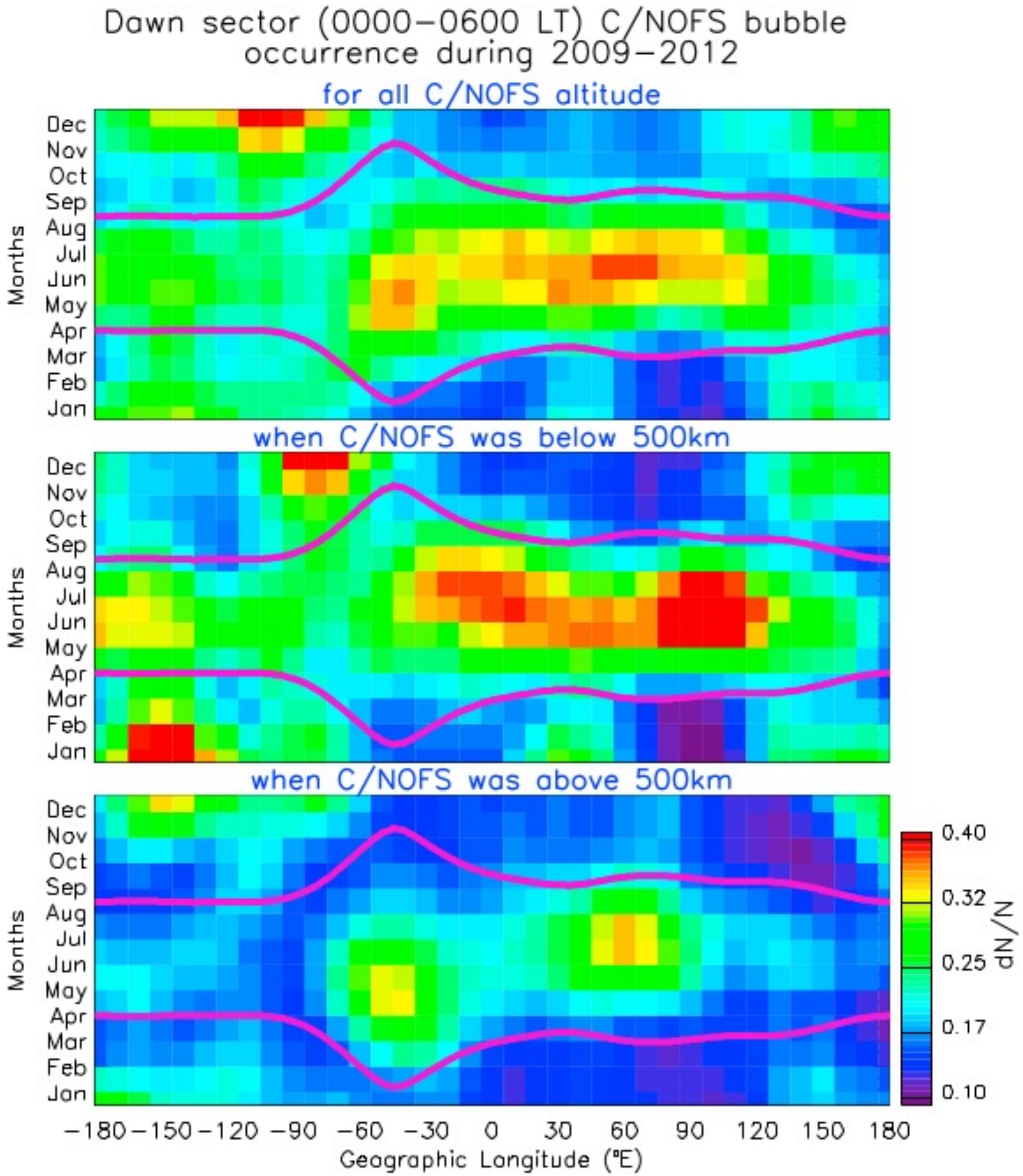

Yizengaw et al., GRL 2013

Post-Midnight Irregularities over Africa

Modeling

C/NOFS Event

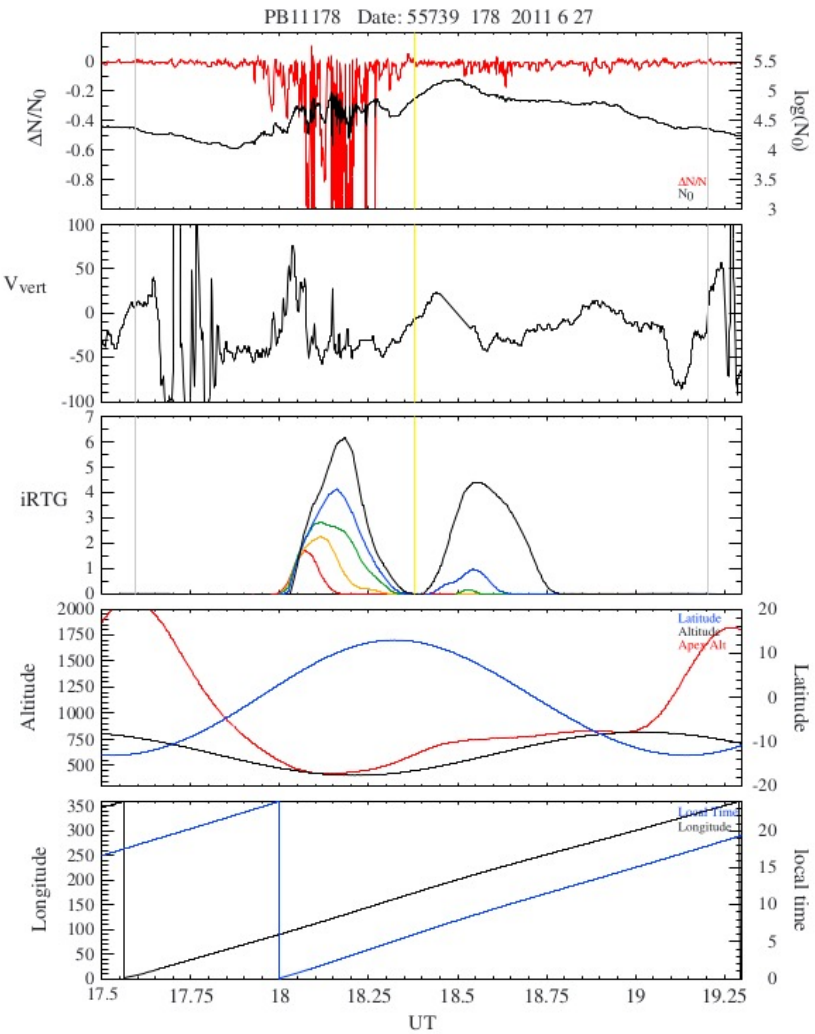

Scintillation modeling with PBMOD using C/NOFS Plasma Drift Climatology

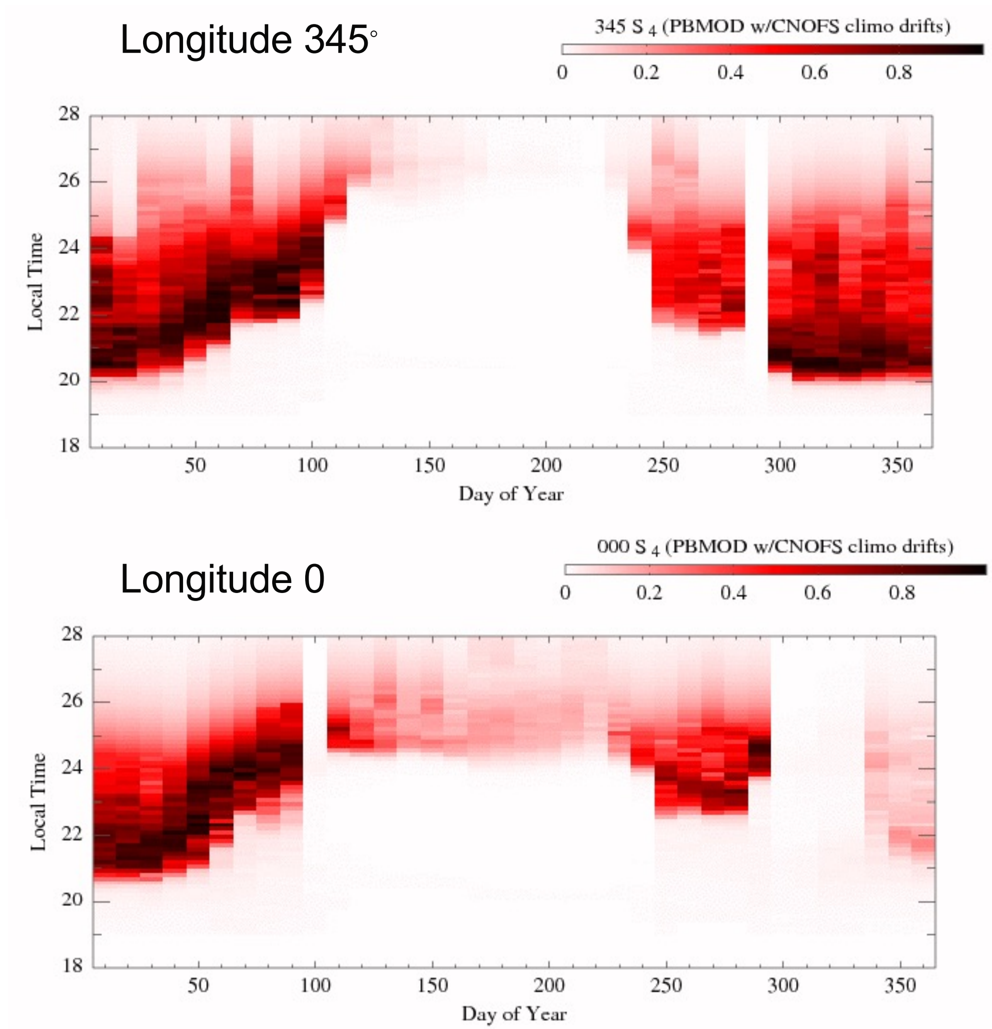

Difficulty: The Uncertainty in Ambient Forecasts

Scintillation sensitively dependent on ambient conditions in ionosphere
Ambient conditions are hard to forecast:

- **Dependent on highly variable external drivers**
- **Highly variable themselves**
- **Difficult to remotely sense in a global way**

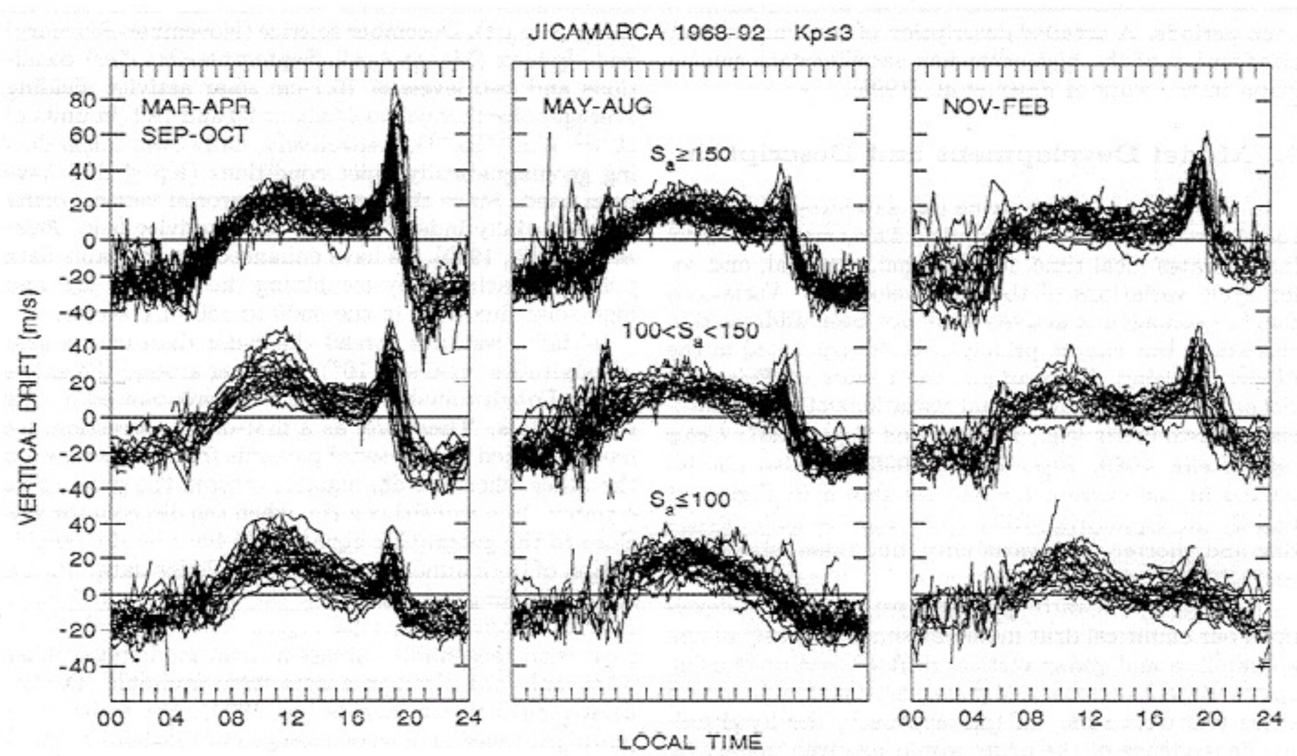

Variability in Plasma Velocity (Scherliess and Fejer 1999)

Influence of Lower Atmosphere
Tides and Gravity Waves Contribute to Daily Variability

Winds in the Whole Atmosphere Model (WAM)

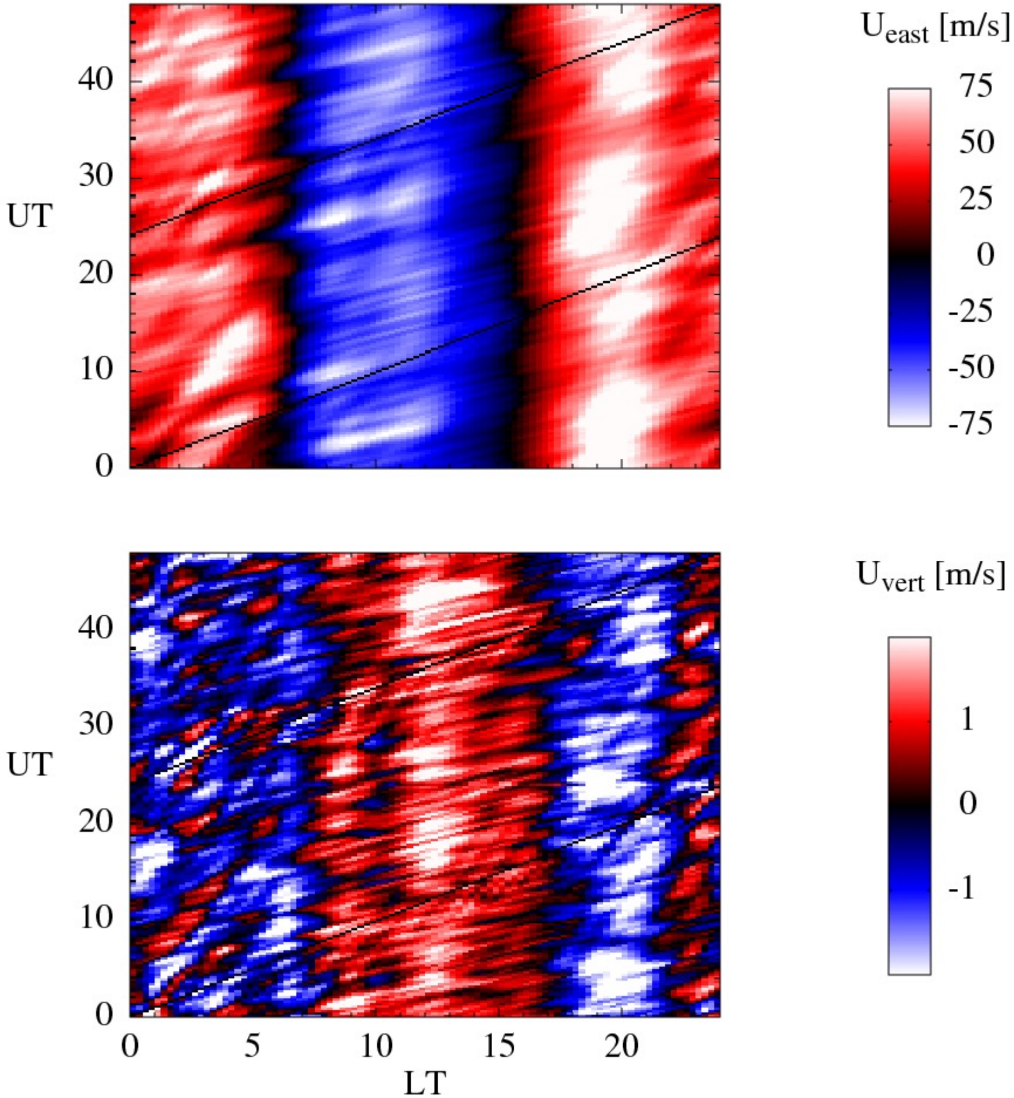

Daily Variability of the RT Growth Rate

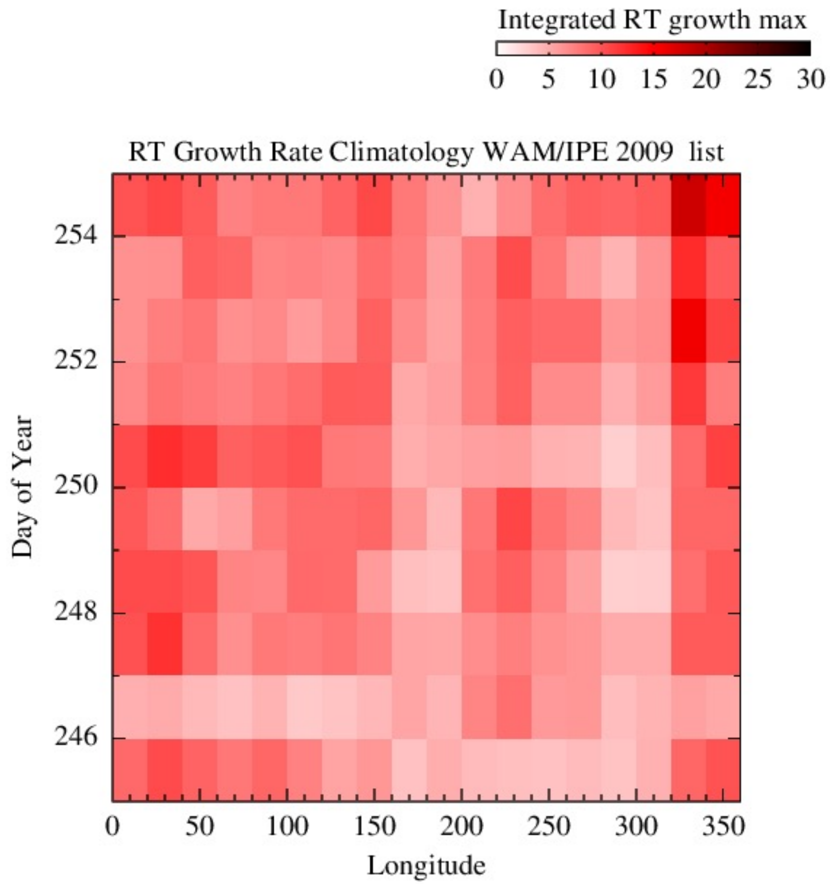

Fuller-Rowell et al., 2008

Sensitivity to Magnitude of Initial Perturbation

With a weaker PRE, a smaller initial perturbation may not lead to bubble development

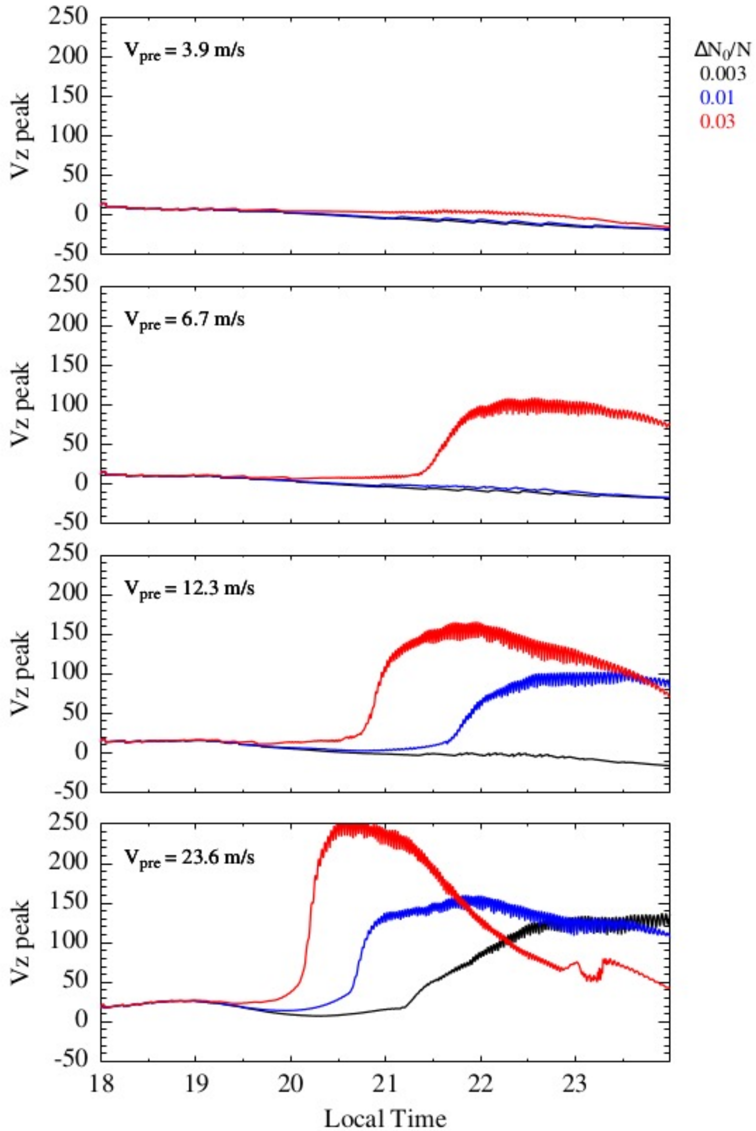

Summary

Equatorial scintillation

- Occurs primarily at night (early evening and early morning)
- Occurs at equinoxes and in other seasons dependent on longitude
- Associated with plasma depletions

Caused by ionospheric plasma turbulence resulting from generalized Rayleigh-Taylor plasma instability

Equatorial ionosphere is unstable when lifted to greater height

- Prereversal enhancement of upward velocity (from neutral wind dynamo)
- Prompt penetration electric fields (during geomagnetically active times)

Summary (continued)

Development of plasma depletions and turbulence is followed using fluid equations for low-latitude ionospheric plasma

Phase-screen model allows spectrum of density irregularities to be used to estimate strength of scintillation

Both climatology and weather are reproduced by models:

- Ambient velocities and densities
- Instability, bubble formation, and scintillation

Great uncertainty still exists in forecasts

- Uncertainty in ambient conditions
- Uncertainty in ‘seed’ plasma fluctuations

Equatorial Plume Issues

- Identify processes controlling structure of plumes
  - Mode structure along field-line
  - Cascade processes, Secondary Instabilities
  - Dissipation processes

- Know ambient environment well enough to apply description of processes
  - Gravity waves & mesoscale structure of ambient ionosphere
  - Winds & wind shear
  - E-region conductivities
  - Electrodynamics of the global ionosphere-thermosphere system

General Reference

The Earth's Ionosphere: Plasma Physics and Electrodynamics (Michael C. Kelley)